Agricultural and Forest Meteorology 346 (2024) 109875

Contents lists available at ScienceDirect

Agricultural and Forest Meteorology

journal homepage: www.elsevier.com/locate/agrformet

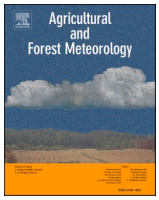

Changes in evapotranspiration, transpiration and evaporation across natural and managed landscapes in the Amazon, Cerrado and Pantanal biomes

B. D'Acunha [a,b,*], H.J. Dalmagro [c], P.H. Zanella de Arruda [d], M.S. Biudes [d], M.J. Lathuillière [e], M. Uribe [f], E.G. Couto [g], P.M. Brando [f], G. Vourlitis [h], M.S Johnson [b,i]

[a] UK Centre for Ecology and Hydrology, Wallingford, UK
[b] Department of Earth, Ocean and Atmospheric Sciences, University of British Columbia, Vancouver, British Columbia, Canada
[c] Programa de Pós-Graduação em Ciências Ambiental, Universidade de Cuiabá (UNIC), Cuiabá, Brazil
[d] Instituto de Física, Universidade Federal de Mato Grosso (UFMT), Cuiabá, Brazil
[e] Stockholm Environment Institute (SEI), Stockholm, Sweden
[f] School of the Environment, Yale University, New Haven, CT, USA
[g] Departamento de Solos e Engenharia Rural, Faculdade de Agronomia e Zootecnia (FAZ), Universidade Federal de Mato Grosso (UFMT), Cuiabá, Brazil
[h] Biological Sciences Department, California State University, San Marcos (CSUSM), CA, USA
[i] Institute for Resources, Environment and Sustainability, University of British Columbia (UBC), Vancouver, British Columbia, Canada

ARTICLE INFO

Keywords:
Land use
Land cover
Tropical ecosystems
Eddy covariance

ABSTRACT

Land-use and land-cover change (LULCC) can dramatically affect the magnitude, seasonality and main drivers of evaporation (E) and transpiration (T), together as evapotranspiration (ET), with effects on overall ecosystem function, as well as both the hydrological cycle and climate system at multiple scales. Our understanding of tropical ecosystem responses to LULCC and global change processes is still limited, mainly due to a lack of ground-based observations that cover a variety of ecosystems, land-uses and land-covers. In this study, we used a network of nine eddy covariance flux towers installed in natural (forest, savanna, wetland) and managed systems (rainfed and irrigated cropland, pastureland) to explore how LULCC affects ET and its components in the Amazon, Cerrado and Pantanal biomes. At each site, tower-based ET measurements were partitioned into T and E to investigate how these fluxes varied between different land-uses and seasons. We found that ET, T and E decreased significantly during the dry season, except in Amazon forest ecosystems where T rates were maintained throughout the year. In contrast to Amazon forests, Cerrado and Pantanal ecosystems showed stronger stomatal control during the dry season. Cropland and pasture sites had lower ET and T compared to native vegetation in all biomes, but E was greater in Pantanal pasture when compared to Pantanal forest. The T fraction of ET was correlated with LAI and EVI, but relationships were weaker in Amazon forests. Our results highlight the importance of understanding the effects of LULCC on water fluxes in tropical ecosystems, and the implications for climate change mitigation policies and land management.

1. Introduction

Tropical ecosystems play a key role in regulating local, regional, and global climate by fixing carbon from the atmosphere, receiving and emitting energy, and returning water to the atmosphere via evapotranspiration (ET) (Lathuillière et al., 2012; Schlesinger and Jasechko, 2014). ET is an important component of the water cycle and surface energy budget, and serves as a key driver for moisture inputs into precipitationsheds through rainfall recycling, especially in South America (Baker et al., 2021; Baker and Spracklen, 2019; Marengo et al., 2016). For instance, Zemp et al. (2014) showed that 18–25 % of the total precipitation over the La Plata basin comes directly from the Amazon basin. Moreover, 9–10 % of the total precipitation over South America is generated through cascading moisture recycling in the region (Zemp et al., 2014).

Land-use and land-cover change (LULCC) can have a significant

* Corresponding author at: UK Centre for Ecology and Hydrology, Wallingford, UK.
E-mail address: brenha@ceh.ac.uk (B. D'Acunha).

https://doi.org/10.1016/j.agrformet.2023.109875
Received 2 July 2023; Received in revised form 21 December 2023; Accepted 24 December 2023
Available online 30 December 2023

impact on ET and affect the hydrological cycle and the availability of water resources. At field and regional scales, conversion of natural vegetation to other land covers typically increases runoff (Miralles et al., 2011; Schlesinger and Jasechko, 2014), alters precipitation regimes (e.g., onset of the wet season, reduction in precipitation) (Fearnside, 2004; Longo et al., 2020), reduces groundwater recharge (Kundzewicz et al., 2008; Montenegro and Ragab, 2012), and increases land surface temperature (Caballero et al., 2022; de Oliveira et al., 2021). Thus, understanding how ET changes across landscapes and management practices is critical to predict the effects of LULCC and mitigate its impacts. Partitioning of ET into evaporation (E) and transpiration (T) and examining their controlling factors and variability across landscapes provides useful information about plant physiological processes, the mechanisms by which they contribute to the global water cycle (Jasechko et al., 2013; Wei et al., 2017), and how these fluxes might be affected by environmental change or anthropogenic disturbances (i.e. LULCC, drought, increases in atmospheric CO_2 concentrations, etc.) (Uribe et al., 2021; Maeda et al., 2017; Xu et al., 2019). In addition, studying T and its contribution to ET can provide important information about land management impacts on water resources. For example, increasing T/ET (i.e., increasing "productive" water flow) has been proposed as a strategy to increase crop yields in agricultural systems, as T is directly coupled to crop growth and yield (Rockström, 2003).

Despite significant efforts towards measuring ET in South America using ground-based observations, such as through the Large-Scale Biosphere-Atmosphere experiment in Amazonia (LBA) (Keller et al., 2004; Restrepo-Coupe et al., 2013), or through remote sensing (Wu et al., 2020; Paca et al., 2019; Baker et al., 2021), seasonal and landscape management effects remain poorly understood in the region primarily due to a lack of ground-based observations that cover a variety of ecosystems, land-uses and land-covers (Caballero et al., 2022; Melo et al., 2012). This lack of field data also leads to uncertain parameterization of hydrological and land surface models, which currently poorly represent the temporal variations of carbon and water fluxes (Maeda et al., 2017; Restrepo-Coupe et al., 2017). This can result in predicting a single trend or driver that might not be representative of the complex mosaic of ecosystems and climates that are found within a regional context (Maeda et al., 2017; Wu et al., 2020). Likewise, getting accurate and disaggregated estimates of T and E remains a challenge due to the large number of factors that influence these fluxes (e.g., climate, soil moisture variability, soil pore size, plant species, photosynthetic capacity, etc.) (Fisher et al., 2017; Mallick et al., 2016), as well as the costs of running a tower network over multiple ecosystems and years. Crucially, land use change impacts on streamflow may mask climate change effects on the water balance (Chagas et al., 2022). For example, deforestation increases streamflow via a reduction in T, which counteracts the reduction in streamflow caused by climate change (Cavalcante et al., 2019; Chagas et al., 2022; Levy et al., 2018). This indicates the importance of detailed inspection of T and E in natural and managed ecosystems.

In this study, we used data from nine eddy covariance towers located across the state of Mato Grosso, Brazil, to investigate how E and T vary within three primary biomes (Amazon, Cerrado, Pantanal) for natural (forest, savanna, wetland) and managed (rainfed and irrigated cropland, pastureland) land uses and land covers. The Amazon, Cerrado, Pantanal biomes have each experienced extensive deforestation and land-use change for cattle grazing and crop production in recent decades to satisfy the increasing global demand for food, fuel and other commodities. Here, we specifically focus on (i) how land-use and land-cover change affects ET, T, E and T/ET within and between biomes, and for natural vs. managed land covers within each biome, (ii) seasonal differences (dry vs. wet seasons) in ET and its components, and (iii) the main drivers of these fluxes at site and regional scales. This study provides additional understanding of tropical ecosystems and expected responses to LULCC through the development of a harmonized dataset that is complementary to previously published multi-site studies focused primarily on the Amazon biome (e.g., Restrepo-Coupe et al., 2013). The achieved expansion of observations into the Cerrado and Pantanal biomes, including both natural and managed ecosystems in each biome, has a great potential to inform hydrological and land surface models, and further improve our understanding of how these systems are likely to respond to ongoing global change processes.

2. Methods

2.1. Study sites

Eddy covariance (EC) and ancillary micrometeorological data (Table S1) were obtained for nine research sites located across the nearly 1×10^6 km^2 Brazilian state of Mato Grosso (Fig. 1, Table 1). The hydroclimates of Mato Grosso present a unimodal rainfall regime with a well-defined dry season and distinct north-south gradients in mean annual precipitation (greater in the north) and dry season length (longer in the south). In Mato Grosso, humid tropical rainforest vegetation is present only in the extreme north of the state. Much of the dense tropical Amazonian forest in Mato Grosso consists of "transitional forest" across a diffuse ecotone between Cerrado savanna forests in the central part of the state and humid tropical forests in the north. The northern portion of the Pantanal is located in the southern portion of Mato Grosso state. The northern Pantanal experiences seasonal flooding each year from overbanking of the river systems and local precipitation (Dalmagro et al., 2018).

We used the following naming conventions for the EC tower sites: the first letter refers to the biome (*A* = Amazon, C = Cerrado, *P* = Pantanal), the second letter refers to the land cover (*P* = pasture, *F* = forest, *A* = agriculture, C = *campo sujo* type savanna). For sites with the same biome and land cover, we used a third letter that refers to the location (*S* = Sinop, *T* = Tanguro, *J* = Jaciara, *L* = Lucas do Rio Verde).

AP (Amazon Pasture) is a cattle pasture located at the Fazenda São Nicolau near Cotriguaçú, converted from humid rainforest within the Amazon biome. **AFS** (Amazon forest Sinop) and **AFT** (Amazon forest Tanguro) are intact "transitional forest" sites located within the Amazon biome. **AA** (Amazon agriculture) is an agricultural site converted from native forest at Fazenda Tanguro. Soybean (*Glycine* max) was grown as a monoculture at AA in 2015 and 2016, planted in December and harvested in March (2015) and April (2016). Millet (*Panicum miliaceum*) was established as a sparse cover crop in 2017 (from March – August). **CC** (Cerrado Campo sujo) is a natural savanna ecosystem located in the Cerrado. The vegetation at this site is locally known as 'Campo sujo', and consists of a woodland savanna dominated by C4 grasses, typical for the Cerrado biome in the region. **CAL** (Cerrado agriculture Lucas do Rio Verde) is an agricultural field located at Fazenda Capuaba in the Cerrado biome (Lathuillière et al., 2018). Fazenda Capuaba uses a double cropping system with soybean planted as the wet season (primary) crop and maize (*Zea mays*) as the dry season (secondary) crop in most years, but also produces other secondary crops (e.g., rice (*Oryza sativa*), and forage crops) based on the crop rotation. The same EC system was used to take simultaneous measurements at two fields in CAL: rainfed (CAL) and irrigated (CALirr). CALirr received 118 mm of irrigation during the dry season and until the onset of the rainy season (from June to September 2016), and was rainfed for the rest of the study period. **CAJ** (Cerrado agriculture Jaciara) is located at Fazenda Nascente, and is also an agricultural site in the Cerrado biome. The farm double crops soybean and maize sequentially within a 12-month period, and follows a typical crop management system for farms in this region (double cropping of soybean (wet season) and maize (dry season) under no-till cultivation). **PF** (Pantanal forest) and **PP** (Pantanal pasture) are sites located in the Pantanal biome. PF is a natural forest located in a national reserve (SESC Pantanal) and is part of a research station managed by the Federal University of Mato Grosso (da Silva et al., 2021; Dalmagro et al., 2019). The site is considered a hyper-seasonal forest, as it experiences annual flooding during the rainy season (October - March) and strong droughts during the extended dry season. Finally, PP is a pasture site used

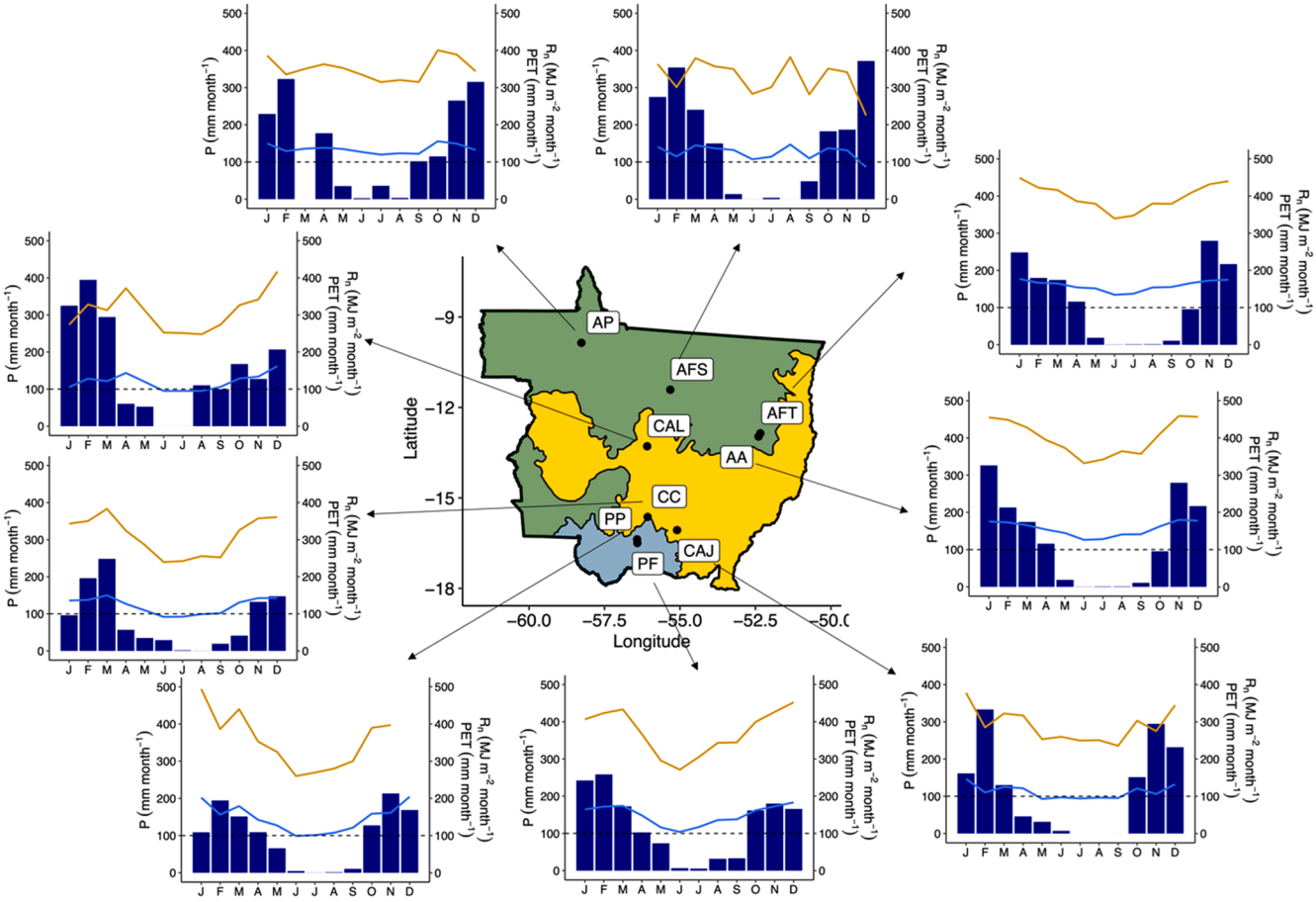

Fig. 1. The figure shows the state of Mato Grosso, Brazil with the Amazon (green), Cerrado (yellow) and Pantanal (blue) biomes and the location of the eddy covariance towers used in this study. AP = Amazon pasture, AFS = Amazon forest (Sinop), AFT = Amazon forest (Tanguro), AA = Amazon agriculture, CAL = Cerrado agriculture (Lucas do Rio Verde), CC = Cerrado campo sujo, CAJ = Cerrado agriculture (Jaciara), PP = Pantanal pasture, PF = Pantanal forest. For each site, monthly precipitation (P in mm month^{-1}, blue bars), net radiation (R_n in MJ m^{-2} month^{-1}, yellow line) and potential evapotranspiration (PET in mm month^{-1}, blue line) are shown.

exclusively for cattle ranching. The pasture is in a state of degradation (Dalmagro et al., 2022). Further details on each site are available in Supplemental Information (Table S1).

2.2. EC data processing

Each EC tower was equipped to provide high frequency measurements of trace gas fluxes (CO_2), latent (LE) and sensible heat fluxes (H), and micrometeorological variables (e.g., ground heat flux (G), net radiation (R_n), air and soil temperatures (T_{air}, T_{soil}), etc.) (Table S2). We worked with half-hourly EC flux data that were provided by each site's operator, and employed a consistent quality assurance and quality control and post-processing procedures for all sites to ensure that all data were treated similarly. Post-processing of EC data was conducted using EddyPro software (version 7.0.6, LI-COR Biosciences, Lincoln, NE, USA) (Fratini and Mauder, 2014). EC data were filtered (i.e., removed) when the analyzer signal strength was below 50 %, as well as for 30-min periods flagged as 'low quality' by EddyPro (QC > 1) after being tested for stationarity and turbulent conditions (Foken et al., 2006). For sites equipped with an open path infrared gas analyzer (i.e., LI-7500A, LI-COR, Lincoln, NE), we also removed fluxes recorded during precipitation events. Because the EC towers at CAL and CAJ were positioned between two adjacent fields, fluxes were assigned to each field based on wind direction. At CAL, fluxes with a wind direction between 0° - 150° were assigned to the rain-fed field (CAL), and fluxes with a wind direction between 150° - 320° were assigned to the irrigated field (CALirr) (Dalmagro et al., 2022; Lathuillière et al., 2018). At CAJ, fluxes with a wind direction from 35° to 220° were assigned to CAJ-1, and from 0 to 30° and 225°–360° were assigned to CAJ-2. As the gross primary productivity (GPP) is used for ET partitioning, the net ecosystem exchange (NEE, estimated as the sum between the CO_2 fluxes and the one-point profile CO_2 storage estimate provided by EddyPro) was also filtered out for periods with insufficient turbulence (low friction velocity, u_*) (Papale et al., 2006). For this, we generated a u_* threshold distribution for each site by bootstrapping the data (200 samples) and estimating the 5 %, 50 % and 95 % percentiles (Pastorello et al., 2020; Wutzler et al., 2018). Only the 50 % percentile was used for further processing and the values are shown in Table S3. The percentage of flux data retained for each site after filtering are shown in Table S3.

After filtering, meteorological and flux (NEE, LE) data from each site were gap filled using the marginal distribution sampling procedure (MDS) (Reichstein et al., 2005), except of LE fluxes at CAL. Due to the multiple fields and crops produced during the study period at CAL, LE at rainfed (CAL) and irrigated (CALirr) fields were gap-filled using the Priestley-Taylor α method (Lathuillière et al., 2018; Vourlitis et al., 2015, 2002).

NEE was then partitioned into GPP and ecosystem respiration (R_{eco}). We used the nighttime method (Reichstein et al., 2005) for all sites except AP where the relationship between R_{eco} and temperature was not sufficiently robust. Instead, we partitioned NEE for AP using the light response curve approach (daytime method) (Lasslop et al., 2010). Both methods (daytime and nighttime) were compared using data from all

Table 1
Information about the study sites. We used the following naming conventions for the EC tower sites: the first letter refers to the biome (*A*= Amazon, C = Cerrado, *P* = Pantanal), the second letter refers to the land cover (*P* = pasture, *F* = forest, *A* = agriculture, C = campo sujo). For sites with the same biome and land cover, we used a third letter that refers to the location (*S* = Sinop, *T* = Tanguro, *J* = Jaciara, *L* = Lucas do Rio Verde).

Site code	Biome	Land use	Location	Coordinates	Study period	Vegetation	MAT (°C)	MAP (mm)	EC system	Measurement height (m)	References
AA	Amazon	Agriculture (rainfed)	Tanguro Ranch, Querencia, MT	12°57′58.4″ S 52°23′53.5″ W	Mar 2015 - Dec 2017	Soybean: 2015–12–05 to 2016–04–07 Soybean: 2016–12–20 to 2017–03–23 Millet: 2017–03–27 to 2017–08–05	25	1770	CO_2/H_2O concentration: Li7200 (Li-COR Inc., Lincoln, NE, USA) 3D Sonic anemometer: USA1 (METEK, Elmshorn, GER)	6	Conte et al. (2019)
AFT	Amazon	Forest (Amazon - Cerrado transition)	Tanguro Ranch, Querencia, MT	12°51′26.1″ S 52°20′15.8″ W	Jan 2015 -Dec 2017	Amaioua guianensis Aubl., Ocotea acutangula Mez., Aspidosperma excelsum Benth., Ocotea guianensis Aubl., Tapirira guianensis Aubl., Micropholis egensis (A. DC.) Pierre, Trattinnickia burserafolia Mart., Sloanea eichleri Schum., Trattinnickia rhoifolia Willd., Pouteria ramiflora (Mart.), Radlk, Trattinnickia glaziovii Swart.	25	1770	CO_2/H_2O concentration: Li7200 (Li-COR Inc., Lincoln, NE, USA) 3D Sonic anemometer: USA1 (METEK, Elmshorn, GER)	36	Brando et al. (2019); Balch et al. (2008)
AP	Amazon	Pasture	Cotriguaçu, MT	9°52′06″ S 58°14′09″ W	Mar 2002 - Jul 2003	Brachiaria brizantha	24.5	2000	CO_2/H_2O concentration: NOAA-ATDD (Oak Ridge, TN, USA) 3D Sonic anemometer: SWS-211/3 K (Applied Technologies Inc., Boulder, CO, USA)	8	Priante-Filho et al. (2004)
AFS	Amazon	(Amazon - Cerrado transition)	Sinop, MT	11°24′44.28″ S 55°19′28.77″ W	Jul 2005 - Jun 2008	Tovomita cf. schomburgkii (Planch and Triana), Protium sagotianum (Marchand), Brosimum lactescens (S. Moore) and Dialium guianense (Aubl.)	24	1940	CO_2/H_2O concentration: Li-7500 (Li-COR Inc., Lincoln, NE, USA) 3D Sonic anemometer: CSAT-3 (Campbell Scientific, Inc., Logan, UT, USA)	42	Vourlitis et al. (2004, 2005)
PP	Pantanal	Pasture	Poconé, MT	16°22′24″ S 56°27′44″ W	Feb 2018 -Feb 2020	Capim mimoso and Brachiaria brizantha (degraded pasture)	25	1213	CO_2/H_2O concentration: Li-7500A (Li-COR Inc., Lincoln, NE, USA) 3D Sonic anemometer: 81,000 (R.M. Young Company	5	Dalmagro et al. (2022)

(*continued on next page*)

Table 1 (*continued*)

Site code	Biome	Land use	Location	Coordinates	Study period	Vegetation	MAT (°C)	MAP (mm)	EC system	Measurement height (m)	References
									Traverse City, MI, USA)		
PF	Pantanal	Forest (seasonally flooded)	Poconé, MT	16°29′53.52″ S 56°24′46.23″ W	Mar 2015 -Jun 2017	Combretum lanceolatum (Combretaceae), Thalia geniculate and Nymphaea sp.	24.9	1213	CO_2/H_2O concentration: Li-7500A (Li-COR Inc., Lincoln, NE, USA) 3D Sonic anemometer: 81,000 (R.M. Young Company Traverse City, MI, USA)	20	Dalmagro et al. (2019)
CC	Cerrado	Campo sujo	Cuiabá, MT	15°43′53.66″ S 56°04′18.81″ W	2011–2014	Brachiara humidicola, Curatella americana and Diospyros hispida A. DC	26.5	1454	CO_2/H_2O concentration: Li-7500 (Li-COR Inc., Lincoln, NE, USA) 3D Sonic anemometer: CSAT-3 (Campbell Scientific, Inc., Logan, UT, USA)	10	Zanella De Arruda et al. (2016)
CAJ	Cerrado	Agriculture (rainfed)	Jaciara, MT	16°04′02″ S 55°05′47″ W	Sep 2019 -Jan 2022	CAJ-1: Soybean: 2019–10–12 to 2020–02–15 Brachiaria/ crotalaria: 2020–03–04 to 2020–07–15 Soybean: 2020–10–20 to 2021–03–06 CAJ-2: Soybean: 2019–10–15 to 2020–02–26 Maize: 2020–02–27 to 2020–06–20 Soybean: 2020–10–17 to 2021–01–20	24.5	1301	CO_2/H_2O concentration: Li-7500A (Li-COR Inc., Lincoln, NE, USA) 3D Sonic anemometer: 81,000 (R.M. Young Company Traverse City, MI, USA)	3.7	–
CAL	Cerrado	Agriculture (rainfed)	Lucas do Rio Verde, MT	13°17′15.03″ S 56°05′17.35″ W	Sep 2015 -Feb 2017	Soybean: 2015–10–28 to 2016–02–11 Maize: 2016–02–13 to 2016–07–13 Brachiaria: 2016–07–14 to 2016–10–04 Soybean: 2016–10–05 to 2017–02–04	26.7	1940	CO_2/H_2O concentration: Li-7500A (Li-COR Inc., Lincoln, NE, USA) 3D Sonic anemometer: 81,000 (R.M. Young Company Traverse City, MI, USA)	3.7	Lathuillière et al. (2018), Dalmagro et al. (2022)
CALirr	Cerrado	Agriculture (irrigated)	Lucas do Rio Verde, MT	13°17′15.03″ S 56°05′17.35″ W	Sep 2015 -Feb 2017	Soybean: 2015–09–29 to 2016–01–13 Rice: 2016–02–01 to 2016–04–30 Beans: 2016–06–14 to 2016–09–22 Soybean: 2016–09–30 to 2017–02–04	26.7	1940	CO_2/H_2O concentration: Li-7500A (Li-COR Inc., Lincoln, NE, USA) 3D Sonic anemometer: 81,000 (R.M. Young Company Traverse City, MI, USA)	3.7	Lathuillière et al. (2018), Dalmagro et al. (2022)

sites, and yielded similar results ($GPP_{nighttime} = 1.1 + 1.1GPP_{daytime}$, $R^2 = 0.65$, $p < 0.001$) (Fig. S1). Therefore, only the results from the nighttime method are presented (except for AP). EC data were processed in R version 4.1.2 (R Core Team, 2021). Filtering, gap-filling, and NEE partitioning were performed using the REddyProc package (Wutzler et al., 2018).

The energy balance of eddy covariance systems and its degree of closure is often used as an indicator of system performance and measurement quality (Culf et al., 2004; Foken, 2008). The energy balance closure at each site was determined using the ordinary least squares regression method (i.e., plot of turbulent fluxes (H + LE) against available energy (Rn - G)), and the energy balance ratio (i.e., the ratio of LE + H and Rn - G). Energy balance results are presented in Table S3. A discussion of data quality and energy balance closure at these sites has been presented in other studies (da Silva et al., 2021; Dalmagro et al., 2019, 2022; Lathuillière et al., 2018; Priante-Filho et al., 2004; Zanella De Arruda et al., 2016). Fluxes were not adjusted to account for the energy imbalance (i.e., energy balance closure was not forced) because of the importance of storage fluxes in some of these ecosystems (i.e., PP, PF), the absence of G measurements at some sites (e.g., PF), and the potential errors in measured G, which can be a large source of uncertainty, particularly in agricultural, grassland and chaparral ecosystems (Wilson et al., 2002; Zanella De Arruda et al., 2016).

2.3. ET partitioning

ET measurements from eddy covariance can be partitioned into T and E using several methods (Nelson et al., 2018; Perez-Priego et al., 2018; Scanlon and Kustas, 2010; Scott and Biederman, 2017; Zhou et al., 2016). However, some of these methods require long-term (Scott and Biederman, 2017) or high frequency data (Skaggs et al., 2018) that were not available at all of our sites. For this reason, we partitioned ET into T and E using two distinct approaches: the underlying water use efficiency (uWUE) method developed by Zhou et al. (2016), and the transpiration estimation algorithm (TEA) (Nelson et al., 2018). Code for both partitioning methods used in this study was obtained from the GitHub repository developed by Nelson (2020).

The uWUE method is based on the estimation of the underlying water use efficiency (*uWUE* in g C $hPa^{0.5}$ kg^{-1} H_2O), defined as:

$$uWUE = \frac{GPP * VPD^{0.5}}{ET} \quad (1)$$

Where *GPP* is the gross primary productivity (g C m^{-2} day^{-1}), *VPD* is vapor pressure deficit (hPa) and ET is evapotranspiration (kg m^{-2} day^{-1}, equivalent to mm day^{-1}).

To obtain the T/ET ratio, two variants of *uWUE* were estimated. The potential *uWUE* ($uWUE_p$), is calculated as the slope of 95th percentile regression between GPP*$VPD^{0.5}$ and ET, and represents the periods when plants attempt to maximize carbon uptake while minimizing water loss. To estimate $uWUE_p$, data that were measured during and at least 2 days after rainfall were removed to ensure that only periods where $T \approx$ ET remain in the datasets. The apparent *uWUE* ($uWUE_a$) is estimated using Eq. (1), and considers all the available data during the study period. The ratio of T/ET can then be calculated as in Eq. (2). Further description of the method can be found in Zhou et al. (2016).

$$\frac{T}{ET} = \frac{uWUE_a}{uWUE_p} \quad (2)$$

The TEA method uses a non-parametric model to estimate plant water use efficiency (WUE) where WUE = GPP/T. The model is first trained using ecosystem water use efficiency (WUE_{eco} = GPP/ET) during periods in which plants are active and the contribution of surface evaporation should be minimal (i.e., growing season, dry periods), and then the trained model is used to predict the WUE for every time step, but this time as GPP/T. Similar to the uWUE method, TEA uses the 75th percentile of the modeled relationship between GPP and ET to estimate T. Further description about the TEA model can be found in Nelson et al. (2018).

In this study, we report T and E as the mean of the values obtained from the two ET partitioning methods, TEA and uWUE. We used this mean as a model ensemble, to be able to compare between biomes and land-uses. The results for the individual partitioning methods are shown in the supplementary information.

2.4. Ancillary data

Environmental variables (net radiation (R_n), photosynthetically active radiation (PAR), soil volumetric water content (VWC) measured at the shallowest depth (0.05–0.10 m), vapor pressure deficit (VPD), precipitation (P), air and soil temperature (T_{air}, T_{soil}), incoming shortwave radiation (SW_{in}), and wind speed (WS)) were measured at each location together with EC data. We also collected data for leaf area index (LAI), enhanced vegetation index (EVI) and the fraction of photosynthetically active radiation absorbed by the vegetation (fAPAR) from remote sensing products described below to evaluate vegetation controls on water fluxes (Nelson et al., 2020; Wei et al., 2017).

2.5. Canopy conductance

To have a better understanding of stomatal control on water fluxes at each study site, we modelled the daytime ($SW_{in} > 10$ W m^{-2}) surface conductance (g_c, m s^{-1}) from the inverted Penman-Monteith equation using the 'bigleaf' package (Knauer et al., 2018).

$$g_c = \frac{LEg_a\gamma}{\Delta(R_n - G) + \rho C_p g_a VPD - LE(\Delta + \gamma)}$$

where LE is the latent heat flux (W m^{-2}), Δ is the slope of the saturation vapor pressure curve (kPa K^{-1}), γ is the psychrometric constant (kPa K^{-1}), C_p is the heat capacity of dry air (J K^{-1} kg^{-1}), ρ is the air density (kg m^{-3}), R_n is the net radiation (W m^{-2}), G is the ground heat flux (W m^{-2}), and g_a is the aerodynamic conductance (m s^{-1}) obtained as:

$$g_a = \left(\frac{WS}{u_*^2} + 6.2u_*^{-0.67}\right)^{-1}$$

where WS is the wind speed at measurement height (m s^{-1}) and u_* is the friction velocity (m s^{-1}).

2.6. Remote sensing data

Remotely sensed data products corresponding to EC flux data were collected for each study site for locations centered on each EC tower. For LAI and fAPAR, we used the MODIS product MCD15A3H version 6, Level 4, which has a temporal resolution of 4 days and a spatial resolution of 500 m (Myneni et al., 2002). EVI was obtained at a temporal resolution of 16-days and a spatial resolution of 250 m from the MODIS product MOD13Q1, version 6, Level 4. All the data were downloaded from Google Earth Engine, using the R package 'rgee' (Aybar, 2022).

2.7. Statistical analysis

Monthly ET, T and E data were normalized across sites by dividing each water flux by the corresponding monthly R_n at each site to account for hydroclimatic variability within and between sites across Mato Grosso. To compare ET, T and E among biomes, land uses and seasons, we used a bootstrap analysis to estimate the 95 % confidence intervals (10,000 sets of random samples with substitution of the observed daily series). Statistical significance was then determined by the degree of overlap between 95 % confidence intervals of the mean value (Efron and Tibshirani, 1994).

To evaluate the relationship between T/ET and different parameters (LAI, EVI, TA, P, VPD) a non-linear least square model was applied using

the 'nls' function from the 'stats' package version 4.3.0 in R.

3. Results

3.1. Climatic differences across sites

The climate data for all sites showed a unimodal rainfall regime, which is representative of Mato Grosso; however, rainfall amounts, and onset and end of the dry season ($P < 100$ mm month^{-1}) varied across sites (Fig. 1, Table S1). AP (Amazon pasture) and CAL (Cerrado agriculture Lucas do Rio Verde) were the sites with the highest precipitation during the study period (P ~ 2000 mm yr^{-1}), while the other sites received less than 1500 mm yr^{-1}. R_n seasonality was similar at all sites, with a decline in radiation during the dry season (corresponding to the austral winter). This decline in R_n was not observed at AP or AFS, where net radiation remained consistent throughout the year. Mean monthly air temperature was also similar at all sites (Fig. S2), with consistent values throughout the year. Mean monthly VPD, however, varied strongly across sites and seasons (Fig. S2). Mean monthly VPD increased at all sites during the dry season, with maximum daily values observed between July and September. CAJ (Cerrado agriculture Jaciara) had the highest VPD of all sites, reaching a maximum monthly value of 33 hPa during the dry season. AP, on the other hand, was the site with the lowest VPD, with a maximum monthly value of ~10 hPa during the dry season. Mean monthly VWC also differed across sites (Fig. S3); PF (Pantanal flooded forest) had the highest monthly mean VWC (VWC = 0.45 m^3 m^{-3}), followed by AP (VWC = 0.35 m^3 m^{-3}), while both AA (Amazon agriculture) and CC (Cerrado savanna) had the lowest monthly mean VWC (< 0.10 m^3 m^{-3}).

3.2. Seasonal patterns of water fluxes

The seasonality of net radiation-normalized ET, T, E, from here on referred to as ET_{norm}, T_{norm} and E_{norm}, are shown in Fig. 2. For Amazon forest sites (AFT and AFS), the magnitude of ET_{norm} was similar during wet and dry seasons, but there was a clear increase from February to June, and then a decrease from June to October, which coincided with most of the dry season period (Fig. 2A). E_{norm} followed a similar trend to ET, except that values were comparable from January to July, and then decreased from July to September (Fig. 2C). T_{norm}, on the other hand, didn't exhibit any seasonality throughout the year at the Amazon forest sites (Fig. 2B). Pasture and agricultural sites in the Amazon (AP and AA) showed a similar seasonality to the forest for ET_{norm}, T_{norm}, and E_{norm}, but with overall lower values (Fig. 3). In addition, the AA agricultural site showed a significant decrease in each of ET_{norm}, E_{norm} and T_{norm} during the dry season (Fig. 3, A to C). The AP pasture site had lower ET_{norm} during the dry season, but there were no significant seasonal differences at this site for T_{norm} or E_{norm} (Fig. 3, A to C).

For Cerrado ecosystems (Fig. 2, D to F), the natural and rainfed agriculture sites had similar seasonality for ET_{norm} and T_{norm}, although the magnitude of these fluxes was greater at the natural CC site. ET_{norm} and E_{norm} were greater at the natural Cerrado savanna than rainfed agriculture in the dry season, but there was no difference when compared to the irrigated agriculture site, or in T_{norm}. During the wet season, ET_{norm} was also greater at the natural savanna compared to the rainfed site, but not the irrigated site (Fig. 3D). T_{norm} and E_{norm} were similar at all Cerrado sites during the wet season (Fig. 3E, F).

In the Pantanal, the seasonal patterns of ET_{norm}, T_{norm}, and E_{norm} were similar for the pasture (PP) and forest (PF) sites (Fig. 2, G to I), but the pasture site PP experienced a marked decrease in each of these fluxes from June to October. These declines were not observed at the natural PF site for which seasonal variations were less pronounced. ET_{norm} and T_{norm} were greater for the natural site compared to the pasture during wet and dry seasons (Fig. 3, G to I). Pasture E_{norm} was greater than the natural forest during the wet season, but not in the dry season (Fig. 3I).

3.3. Magnitude of ET, T, and E

The magnitude of ET, T and E is shown in Table 2. In terms of ET, The natural sites in the Amazon and Pantanal biomes (AFT, AFS and PF) had the highest values, all above 1000 mm yr^{-1}. In contrast, the lowest ET values were observed at the Cerrado and Amazon agricultural sites (CAJ

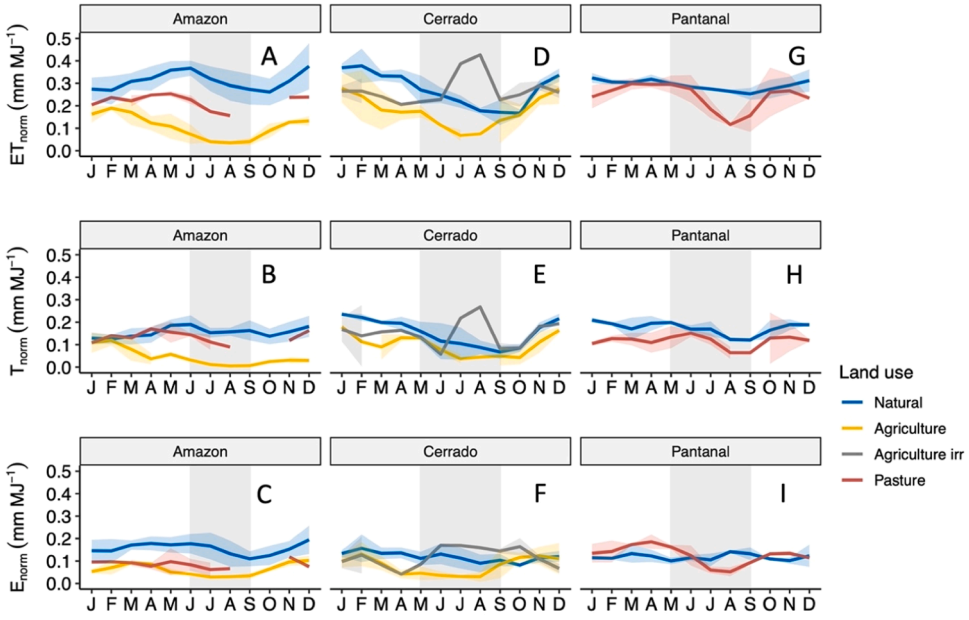

Fig. 2. Monthly means (lines) ± 1 standard deviations (shaded areas) of net radiation-normalized ET (ET_{norm}, mm MJ^{-1}), T (T_{norm}, mm MJ^{-1}), and E (E_{norm}, mm MJ^{-1}) for each biome and land use (Amazon, A to C; Cerrado, D to F; Pantanal, G to I). Blue lines represent natural ecosystems (in the Amazon: the average of AFS and AFT, in the Cerrado: CC, and in the Pantanal: PF), yellow and gray lines represent rainfed (in the Amazon: AA, in the Cerrado: the average of CAJ and CAL) and irrigated agriculture (CAJ), respectively, and the red line represents the sites that are used for cattle pasture (in the Amazon: AP, in the Pantanal: PP). The vertical gray shaded area shows the dry season for each site, determined as $P < 100$ mm month^{-1}. Means ± 1 SD were computed on a monthly basis for sites with multiple years of monthly data.

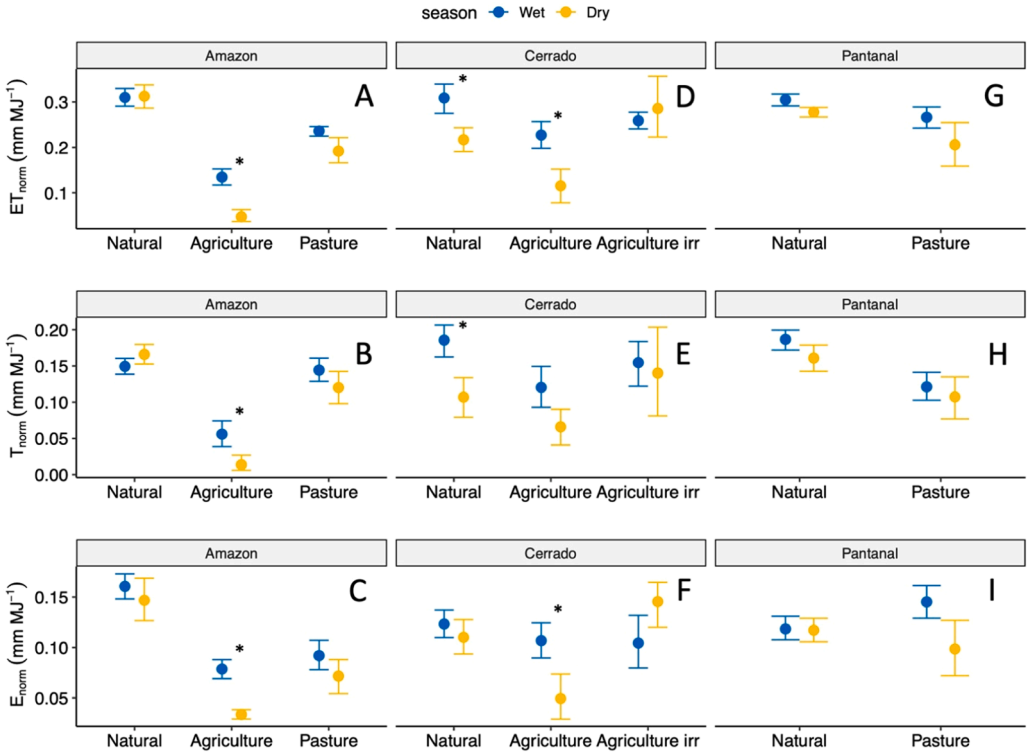

Fig. 3. Net radiation-normalized ET (ET_{norm}, mm MJ^{-1}), T (T_{norm}, mm MJ^{-1}), E (E_{norm}, mm MJ^{-1}), and T/ET for each biome (Amazon, A to C; Cerrado, D to F; Pantanal, G to I) and land-use during wet (blue) and dry (yellow) seasons. The values consider the whole study period at each site (Table 1). Data for natural Amazon forest includes both AFT and AFS. Data for Cerrado Agriculture includes both rainfed CAJ and CAL sites. Dots indicate the mean values. The error bars show the 95 % confidence intervals (CI) estimated via bootstrap analysis. Asterisks indicate significant differences determined by the overlap between the 95 % CI of the mean values.

Table 2
Magnitude of ET, T and E (estimated via TEA and uWUE) for each location and year.

Year	Site	ET (mm)	T_{TEA} (mm)	T_{uWUE} (mm)	T_{mean} (mm)	E_{TEA} (mm)	E_{uWUE} (mm)	E_{mean} (mm)
2015–2016	AA	437	192	134	163	245	303	274
2016–2017	AA	473	240	131	185	234	342	288
2005–2006	AFS	1067	597	493	545	470	574	522
2006–2007	AFS	1067	630	445	537	437	623	530
2015–2016	AFT	1522	817	594	705	705	928	816
2016–2017	AFT	1570	805	633	719	766	938	852
2002–2003	AP	688	465	396	430	224	292	258
2019–2020	CAJ	455	284	262	273	171	193	182
2015–2016	CAL	717	470	290	380	247	426	336
2015–2016	CALirr	952	624	433	528	328	519	423
2011–2012	CC	847	636	323	479	211	524	367
2012–2013	CC	949	624	376	500	324	573	735
2015–2016	PF	1134	745	547	646	389	587	488
2016–2017	PF	1219	875	610	742	344	609	476
2018–2019	PP	1119	782	374	578	337	745	541
2019–2020	PP	832	487	202	344	344	630	487

and AA), with ET values of 455 mm yr^{-1} for CAJ in the 2019–2020 study period, and ET = 437 mm yr^{-1} and 473 mm yr^{-1} for $AA_{2015–2016}$ and $AA_{2016–2017}$, respectively. Likewise, AA and CAJ had the lowest T values of all sites ($T < 300$ mm yr^{-1}). These values were less than half of the T values observed at the natural Amazon and Pantanal sites. CALirr had similar T and ET to the natural Cerrado site (CC) and the natural Amazon forest (AFS). In terms of E, AFT had the highest E ($E = 834$ mm yr^{-1}) and CAJ, AP and AA had the lowest E (182 mm yr^{-1}, 258 mm $yr^{-}1$ and 281 mm yr^{-1} for CAJ, AP and AA, respectively).

3.4. Transpiration to evapotranspiration ratio (T/ET)

For natural Amazon forest sites (AFT, AFS), we observed that T/ET (the ensemble of both methods) significantly increased from a mean T/ET of 0.48 ± 0.08 (mean ± 1 SD) in the wet season to 0.54 ± 0.09 in the dry season (Fig. 4A, I), whereas the opposite was observed for the AA agriculture site decreasing from a mean T/ET of 0.37 ± 0.21 for the wet season (with soybean) to 0.23 ± 0.17 during the dry season (without soybean) (Fig. 4B, I). T/ET from Amazon agriculture (AA) was significantly lower than Amazon natural forest during wet and dry seasons. We found no significant differences at the pasture site (AP) between seasons (T/ET ~ 0.61 for both seasons), but T/ET at the pasture was significantly

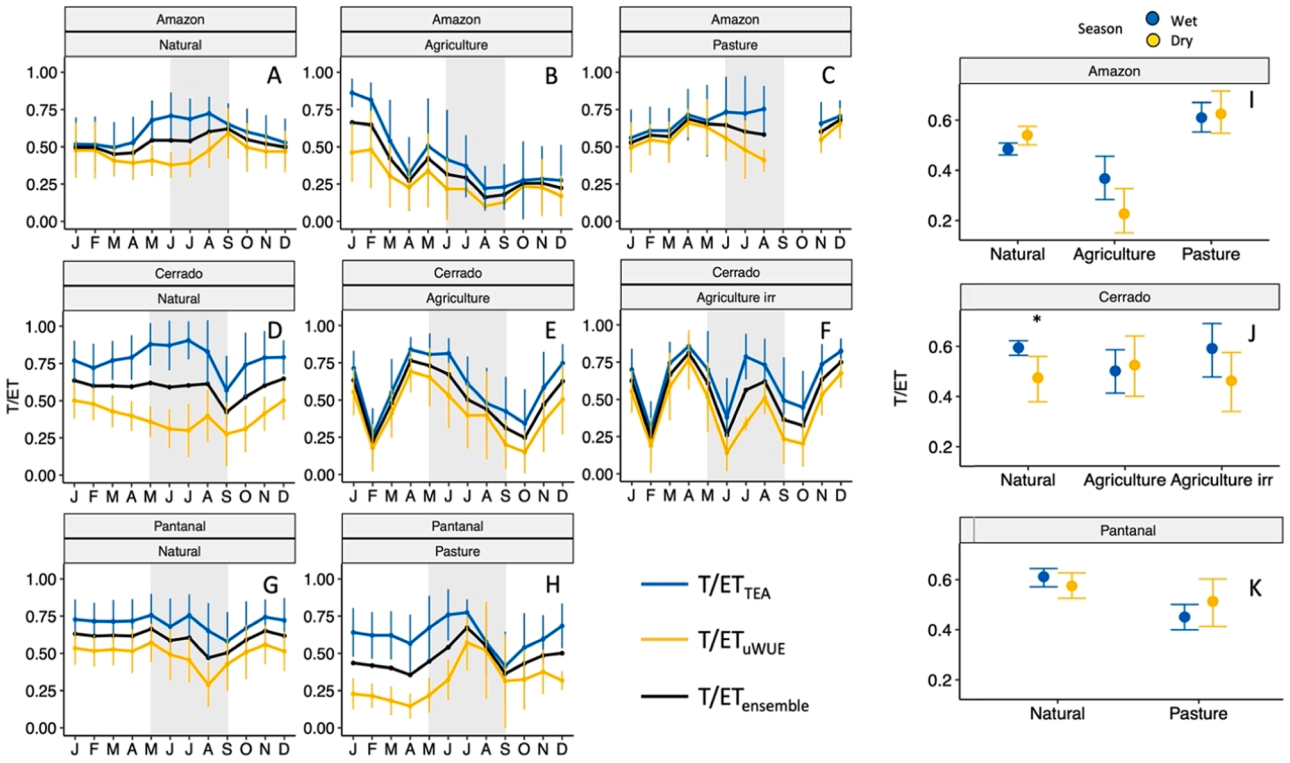

Fig. 4. Left: Monthly means of T/ET for each land use within the Amazon (Natural: AFT, AFS; Agriculture: AA, Pasture: AP) (A to C), Cerrado (Natural: CC; Agriculture: CAL, CAJ) (D to F) and Pantanal (Natural: PF, Pasture: PP) (G, H) biomes. The blue line shows the T/ET estimated using the TEA method, the yellow line shows the T/ET estimated via the uWUE method and the black line shows the ensemble T/ET. The error bars show ± 1 standard deviation. Right: Wet (blue) -Dry (yellow) seasonal differences in T/ET for each biome and land use (I to K). Dots indicate the mean values. The error bars show the 95 % confidence intervals (CI) estimated via bootstrap analysis. Asterisks indicate significant differences determined by the overlap between the 95 % CI of the mean values.

higher than both the natural and agricultural sites in the Amazon (Fig. 4C, I).

In the case of the Cerrado biome, we found that T/ET was higher during the wet season at the natural site compared to the dry season (T/ET was 0.59 ± 0.06 for the wet season, and 0.47 ± 0.19 for the dry season), but there was no seasonal difference in T/ET at the agricultural sites (Fig. 4J). T/ET for the irrigated site was 0.59 ± 0.2 during the wet season, and 0.46 ± 0.16 during the dry season, and T/ET for the rainfed agriculture had lower, but not statistically significant T/ET values (0.50 ± 0.22 and 0.52 ± 0.21, for wet and dry seasons, respectively) (Fig. 4, D to F). Finally, in the Pantanal biome, we observed significantly higher T/ET values at the PF natural site (0.61 ± 0.08) than in the PP pasture site during the wet season (0.45 ± 0.11) (Fig. 4G, H, K).

At the annual scale, T/ET had a mean of 0.53 ± 0.07 considering all biomes and land uses (Table S4). The highest annual T/ET value was observed at the Amazon pasture (0.62), and the lowest value was observed at the Amazon agriculture site (0.40).

3.5. Comparison of TEA and uWUE methods

In general, the TEA method estimated higher T/ET values compared to the uWUE method (Fig. 4). Considering all the study sites, the daily mean T/ET using the TEA method was 0.63, whereas it was 0.42 for the uWUE method. The biggest overall differences between the methods were observed at PP ($T_{TEA}/ET = 0.64$, $T_{uWUE}/ET = 0.32$), followed by CC ($T_{TEA}/ET = 0.79$, $T_{uWUE}/ET = 0.40$), where the results from TEA were almost twice the values estimated using uWUE. The smallest differences in T/ET between the methods were observed at AFS ($T_{TEA}/ET = 0.56$, $T_{uWUE}/ET = 0.47$), AP ($T_{TEA}/ET = 0.68$, $T_{uWUE}/ET = 0.56$) and CAJ ($T_{TEA}/ET = 0.55$, $T_{uWUE}/ET = 0.44$), where daily mean TEA values were about 1.2 times higher than uWUE.

In terms of seasonality, both methods followed a similar pattern for the agricultural sites in each biome, with higher values observed during the crop growing season. The biggest differences between the methods were observed during the dry season. For example, for both natural Amazon and Cerrado natural ecosystems (AFT, AFS, CC), T/ET_{uWUE} decreased, whereas T/ET_{TEA} increased slightly. The opposite was observed at PP, where the biggest differences between T/ET_{uWUE} and T/ET_{TEA} occurred during the wet season, and similar values were observed during the dry season.

3.6. Relationship between T/ET and micrometeorological variables

We observed that sites that had lower LAI or EVI, generally had lower mean values of T/ET (Fig. 5). However, this was not always the case. Amazon forests had higher LAI than the other sites (Fig. S4), but T/ET for AFS and AFP was lower than the Pantanal forest (PF) site as well as for some of the agricultural sites. Moreover, there seems to be little to no correlation between T/ET from the Amazon forest sites and LAI values (Fig. 5). In addition, we found that the relationship between T/ET and other environmental drivers (TA, VPD, and P) was different depending on the method used to estimate T/ET (Figs. S6, S7), but some trends were consistent. For example, at agricultural sites, both T/ET_{uWUE} and T/ET_{TEA} significantly decreased with increasing air temperature. The same was observed at natural Cerrado ecosystems. For natural Amazon forests, neither method showed a significant relationship between T/ET and T_{air}.

We also observed that T/ET tended to remain constant with VPD at low VPD values (< 10 hPa), and then decreased at higher levels of VPD (> 10 hPa) at most sites, with the exception of Amazon pastures (for both uWUE and TEA), natural Amazon forests (using uWUE), and natural Cerrado and natural Pantanal ecosystems (using TEA). Finally, we found a significant relationship between T/ET and P at natural Cerrado and Pantanal pasture ecosystems (using uWUE) (increasing T/ET with

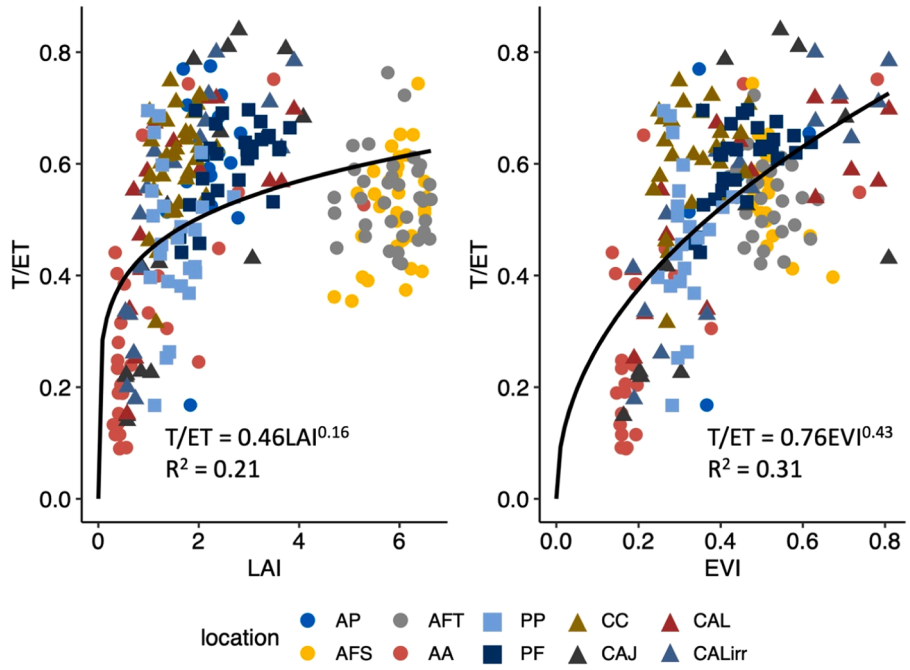

Fig. 5. Relationship between monthly T/ET and VWC, LAI and EVI for each location in this study. The black line shows the best fit using a nonlinear least squares model.

increasing P) and between T/ET and P at natural Amazon forests (using TEA) (decreasing T/ET with increasing P) (Figs. S6, S7).

3.7. Analysis of canopy conductance (g_c)

The canopy conductance (g_c, m s^{-1}) varied in magnitude across biomes, land uses and seasons (Fig. 6, I to K). In the Amazon biome, we found significant differences between wet and dry seasons for all the sites (with higher g_c in the wet season), the largest differences were observed in the Amazon forests, were g_c was almost four times larger in the wet season compared to the dry season (Fig. 6H).

In the Cerrado biome (Fig. 6J), the natural savanna had significantly

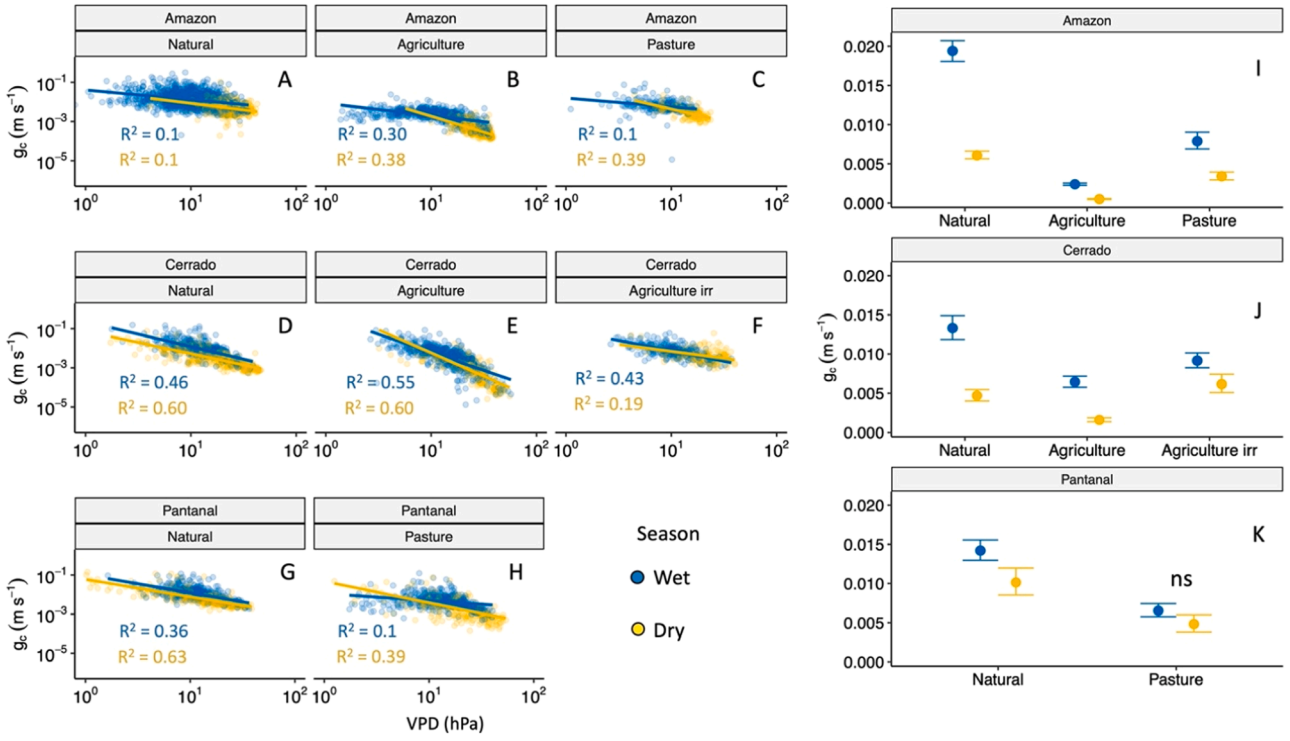

Fig. 6. Left: relationship between mean daytime canopy conductance (g_c, m s^{-1}) and mean daytimeVPD (hPa) for Amazon (A to C), Cerrado (D to F) and Pantanal (G, H) biomes during wet (blue) and dry (yellow) seasons. The values were aggregated into daily timesteps. All the relationships had a p value < 0.001. Right: Wet (blue) and Dry (yellow) seasonal differences in g_c for each biome and land-use. Dots indicate the mean values. The error bars show the 95 % confidence intervals (CI) estimated via bootstrap analysis. ns: not significant.

higher g_c during the wet season compared to the dry season and to the managed sites. Canopy conductance was also higher during the wet season at the rainfed and irrigated agricultural sites, but the seasonal differences were smaller at the irrigated site compared to both the natural and rainfed sites.

Finally, we observed seasonal differences in g_c in the Pantanal forest site, with higher values during the wet season (Fig. 6K). We found no significant differences in g_c at the pasture site, although values were lower than the forest site. In general, we found that g_c was higher at the natural sites compared to the managed sites for both wet and dry seasons.

We also found that the relationship between g_c and VPD depended on season and land use. In general, we found that g_c decreased with increasing VPD and that the relationship was stronger during the dry season (Fig. 6, B, C, D, E, G, and H). However, this was not the case for the natural sites. In the Amazon, we only found a weak relationship between gc and VPD during wet or dry seasons (Fig. 6A). In the Cerrado, the irrigated agricultural site had a stronger relationship between gc and VPD during the wet season compared to the dry season ($R^2 = 0.43$ and $R^2 = 0.19$ for wet and dry seasons, respectively) (Fig. 6F). Finally, in the Pantanal pasture, there was a strong significant relationship between g_c and VPD during the dry season (R^2 =0.39), but only a weak relationship during the wet season ($R^2 = 0.1$) (Fig. 6H).

4. Discussion

4.1. Changes in seasonal patterns of ET, T, and E with landscapes

Our analyses of ET and its components across natural and managed ecosystems in the Amazon, Cerrado and Pantanal biome confirm that LULCC modify the magnitude and seasonality of water fluxes, with managed agroecosystems exhibiting lower fluxes (Fig. 3), a more marked seasonality (i.e., steeper decline during the dry season) (Fig. 2) and a stronger correlation with plant phenology (e.g., LAI, EVI) (Fig. 5), compared to the natural ecosystems. Restrepo Coupe et al. (2013) provide evidence of seasonality in the Amazon, either from photosynthesis (near Manaus) or soil water availability (Southern Amazonia) seasonality due to a more extended dry season. This study provides an extension of the sites described in Restrepo Coupe et al. (2013) with an increasing dry season (Cerrado) and increased water availability in the Pantanal where soils can remain saturated for months into the dry season (Fig. S3). This additional soil water helped maintain higher E levels at the beginning of the dry season for Pantanal sites, compared to the Cerrado.

Amazon forests sites experienced a decline in ET and E during the dry season, but T did not decrease during this period (Fig. 3). Unlike cropland and pasture, Amazon forests have deep roots that can access deep soil water reserves during the dry season (Nepstad et al., 1994; Vourlitis et al., 2011), and therefore can maintain high transpiration rates throughout the year (Staal et al., 2020). Moreover, plant stomata could also play a biotic control in maintaining or suppressing T during the dry season. Across Amazonian sites, Costa et al. (2010) noted more monthly variability in stomatal conductance for Southern Amazonia (corresponding to the most northern region of sites used in the present study). In this study we found that wet season g_c was significantly higher than dry season g_c at the natural Amazonian sites. However, changes in VPD were only able to explain 10 % of the variation in g_c (Fig. 6). This agrees with previous studies in the Amazon, that found that tropical forests can maintain high T rates during the dry season, even at elevated VPD levels (Choat et al., 2012; Green et al., 2020). Moreover, Vourlitis et al. (2008) found that canopy structural properties were more important than direct water limitations in controlling T during the wet-dry season transition in a Southern Amazonia forest. This was because the trees had access to stable water reserves during the dry season. We also observed similar variability in T for forested Cerrado and Pantanal ecosystems in the dry season with a more pronounced drop in T for forest sites in those biomes (compared to steadier E) as compared to the Amazon forest sites. Moreover, we note a substantial decrease in E in the dry season in the Amazon, which in turn is caused by less available soil moisture in the near surface (Fig. S3) (Baker et al., 2021; da Rocha et al., 2009). The decline in dry season E for Amazon forests is in contrast with the Cerrado forest which had a small decline in E over the dry season, and the Pantanal forest site which showed no dry season decline in E, likely due to remaining soil moisture from the annual flood cycle (Fig. 3). These differences in seasonality between T and E suggest stronger stomatal control in the Cerrado and Pantanal ecosystems due to elevated VPD, compared to the Amazon, where both T and E decrease with water availability. This can also be observed in Fig. 6, where VPD exerts a stronger control on g_c in Cerrado and Pantanal natural sites, compared to the natural Amazonian sites. Moreover, all managed sites exhibited a correlation between g_c and VPD during the dry season.

Managed sites also showed a stronger correlations between water fluxes and EVI and LAI, as both remotely sensed data products are related to vegetation cover and crop cycle lengths (Daughtry et al., 1992; Kira et al., 2016). During the growing season (November - April), water fluxes remain similar to the ones observed at natural sites, but suddenly drop upon crop harvesting. Our results also show that management practices, like irrigation, can affect the magnitude and seasonality of water fluxes, with the highest ET and E observed during the dry season at the irrigated site, while both the natural and rainfed sites experienced the lowest values around the same time. The additional peaks in ET and T observed at the irrigated Cerrado site (but not at the natural nor rainfed Cerrado sites) coincided with the planting of irrigated bean (from June to September) (Lathuillière et al., 2018). For the irrigated agricultural site CALirr, 118 mm of irrigation was applied during the dry season, in addition to a mean annual precipitation of 1800 mm for the site.

4.2. Expected changes in E and T with LULCC

It has been widely reported that conversion of Amazon forests to pasture or agriculture significantly reduces the magnitude of ET (Baker et al., 2021; Baker and Spracklen, 2019; de Oliveira et al., 2018). The lower ET values we observed for the Amazon rainfed agricultural site (AA) (Table 2) are related to site management and corresponded to the period for which only one crop was planted per year with no additional management between harvest and the next cropping cycle (except for 2017, when millet was sparsely planted as a cover crop after the soybean) (Table 1). The Amazon pasture site (AP) also had a single (perennial) crop during the study period (*Brachiaria*), so the soil remained covered throughout the study period, but ET, T and E were lower than the natural sites (Table 2). Adding a second crop after soybean (e.g., maize) for AA would likely result in higher levels of T and ET during parts of the dry season (maize crop cycle is usually 120 days, from February to June) and increase food production at the same time (Dalmagro et al., 2022). The viability of moving to a double cropping system in the Amazon's cropland areas will depend on water availability throughout the dry season for the second crop.

The effects of LULCC on ET and its components for the Cerrado are less well established, with studies showing contrasting results. Here, we found that LULCC decreased ET and E during the dry season, which agrees with previous studies that show that ET decreases with conversion of natural vegetation to agricultural land (Nóbrega et al., 2017; Salazar et al., 2015), especially dry season ET when crop growth is limited by the lack of water (Caballero et al., 2022). On the other hand, Uribe et al. (2021) found increasing T during the dry season, and Oliveira et al. (2015) and Loarie et al. (2011) found that annual ET increased when converting natural vegetation to either agricultural or pasture areas. They hypothesized that this increase could be due to i) the conversion of pasture to crops that have similar ET to natural vegetation (e.g., sugarcane), ii) an increase in evaporative demand due to climate change (i.e., rising temperatures, CO_2 concentrations), and iii) the

creation of reservoirs or use of irrigation (Sterling et al., 2012). Although irrigation is still not a widespread practice in the region, there is an increasing body of evidence that suggests that this practice may increase agricultural production in the region without further land use conversion by enabling a third crop cycle during the dry season, as well as increasing water recycling to the atmosphere (Jaramillo et al., 2020; Lathuillière et al., 2016, 2018). This was also observed in this study, where CALirr had similar ET and T ratios to the natural Amazon forest and Cerrado sites (Table 2). However, further studies are needed to understand how irrigation could affect groundwater or other water sources in the region that could be used for this practice to avoid affecting the quantity and quality of freshwater resources.

Information about the effects of LULCC in the Pantanal is much more limited than in the Amazon or Cerrado biomes, even though recent studies indicate that the frequency of extreme events is increasing in the area and that climate change and LULCC will likely lead to hotter and drier conditions in the Pantanal, affecting its role in the global carbon budget, its hydrology and potentially reducing its biodiversity (da Silva et al., 2021; Dalmagro et al., 2018; Garcia et al., 2021; Marengo et al., 2016). Our results suggest that conversion of natural Pantanal vegetation to pasture can significantly decrease ET during the dry season, mostly through a significant reduction in T because of the dry conditions that the area experiences (Figs. 3, 6, Table 2).

4.3. T/ET estimates

Although the ratio of T to ET is a key parameter for understanding the role of vegetation in moisture recycling to the atmosphere, it remains largely unconstrained due to the difficulty in directly measuring T and ET (Fatichi and Pappas, 2017; Fisher et al., 2011). Using LAI to model T/ET, Wei et al. (2017) found that global T/ET is about 0.57 ± 0.07. A synthesis study by Wang et al. (2014) found that T contributes 0.38 – 0.77 of ET, and isotopic data indicate T/ET values from 0.3 to 0.8 (Coenders-Gerrits et al., 2014; Good et al., 2015). In this study, T/ET had a mean of 0.53 ± 0.07 considering all biomes and land uses, which agrees with the estimates presented in previous studies using different methodologies. However, our annual estimate of T/ET for tropical forests (0.50 ± 0.01) is much lower than what was estimated in previous studies (Leopoldo et al., 1995; Salati and Vose, 1984; Shuttleworth, 1988), who found that Amazon forests in Manaus, Brazil had, on average a T/ET of 0.76. This difference could be due to methodological reasons, as the previous studies used different models coupled with site meteorological observations to determine both T and ET. Many of these studies also rely on the estimation of interception by measuring canopy throughfall and stemflow, which can be very challenging and may introduce large systematic errors (Shuttleworth, 1988). In addition, the difference in T/ET could be due to the longer dry season lengths at our study sites. Both Amazon forests in this study (AFS and AFT), located in south and southeast Amazonia and considered "transitional forests" along the Cerrado-Amazon ecotone, receive less precipitation, and experience a stronger seasonality than other forest sites located in northern Amazonia (e.g., near Manaus). For example both AFT and AFS experience, on average, 5 months per year with $P < 100$ mm month^{-1}, while a forest site near Manaus used in other research only experiences 1 month of $P < 100$ mm month^{-1} (Restrepo-Coupe et al., 2013; Signori-Müller et al., 2021). The water limitation that our forest sites experienced also leads to reduced ET via a reduction in T from biotic control (stomata).

T/ET is generally higher in wetter climates, and lower in arid and semi-arid ecosystems, which could explain the lower T/ET observed at the Amazon forest sites (AFT and AFS) relative to values reported for central Amazonia (Schlesinger and Jasechko, 2014). However, we note that as higher VWC does not always lead to higher T/ET, such as in the Pantanal where a greater VWC can increase E, particularly if the vegetation is not adapted to flooding conditions (e.g., the PP pasture site), resulting in lower T/ET due to vegetative constraints. These contrasting results highlight the importance of increasing the number of study sites that span across the multiple microclimates and vegetation types to have better understanding of the variability of T/ET in the region. Another possible explanation for differences in T/ET values between the present and prior studies could be related to the uncertainty in ET partitioning, which is discussed in the next section below.

Comparing all the sites, our results indicate that T/ET didn't vary substantially across biomes, but there were significant differences depending on LULCC. Previous studies have also shown that there is little global-scale variability across biomes in terms of T/ET (Fatichi and Pappas, 2017; Nelson et al., 2020; Paschalis et al., 2018). This could be explained by the lack of differentiation among controls on T and ET. As both T and ET are driven by similar climactic, edaphic and vegetative factors, the effect of these controls can cancel out when looking at T/ET. Another hypothesis is related to the compensation observed between soil evaporation and canopy interception. With higher vegetation cover (and higher LAI), the role of interception increases, and soil evaporation decreases as less water reaches the soil (Fatichi and Pappas, 2017). Thus, T/ET can remain constant even as the sources of E shift (e.g., canopy interception vs. soil evaporation). Another potential explanation refers to plant adaptation to local climate to maximize water use during dry conditions (Fatichi and Pappas, 2017; Nelson et al., 2020). A study by Ohkubo et al. (2023) in a tropical peat swamp forest found that drying conditions reduced T, but it subsequently recovered as the trees acclimated to the dry environment. Managed sites, on the other hand, have vegetation that might not be adapted to local conditions, and that rely more on management practices, or that vary substantially in response to the crop that is being used; therefore T/ET may be directly linked to management factors including crop water use dynamics, cropping season lengths (which vary by crop type), and irrigation (if any).

The differences observed in the Pantanal for ET and its components could also be related to the amount of open water at the sites. Eichelmann et al. (2022) found that T contributed to 70–75 % of ET in a densely vegetated wetland, but this percentage decreased considerably at other locations with more open water surfaces and lower vegetation density, reaching values lower than 15 % at some sites. Previous studies have reported a strong influence of vegetation cover over T/ET values at different timescales and for several vegetation types (Berkelhammer et al., 2016; Scott et al., 2021; Wang et al., 2014; Zhou et al., 2018). In our study, we found that T/ET was correlated with LAI at most sites, except for the Amazonian forests. This lack of relationship for some sites in our study could be related to the use of LAI from remote sensing products instead of field LAI measurements as there could be a spatial mismatch between what is captured by the satellite vs. what the eddy covariance tower measures (Nelson et al., 2020). However, other studies suggest that LAI is only a good predictor of T/ET below a specific LAI threshold. That is, T/ET increases rapidly as LAI increases until reaching this LAI threshold, and afterwards LAI no longer drives T/ET (Sun et al., 2019). In addition, Paschalis et al. (2018) showed that at ecosystems with natural vegetation, and where LAI > 1, there is a negligible dependence of T/ET on LAI, and indicated that agricultural sites don't follow this pattern because crops are not in equilibrium with local climate (i.e., not adapted to local conditions) and depend more on management practices (e.g., irrigation, fertilization, etc.).

VWC could also be an important predictor of T/ET. Cui et al. (2020) found that surface soil water content was the most important control of T/ET at the seasonal scale in an alpine meadow ecosystem, with LAI only playing a secondary role. Likewise, Zhou et al. (2016) found that seasonal variation of T/ET in evergreen forests was mainly attributed to environmental factors, because intra-annual variation of vegetation cover is small for these forests. We also note the strong correlation in the present study between EVI and T/ET at all sites, which agrees with previous findings from Zhou et al. (2016) who found a $R^2 = 0.85$ for the relationship between EVI and T/ET.

4.4. Uncertainty in T, E and T/ET estimates and study limitations

The uncertainty in our measurements derives mainly from four sources: (i) NEE filtering, gap-filling, and partitioning into GPP and *Re*, (ii) energy balance closure, and (iii) the methods used for ET partitioning into T and E. Both ET partitioning models used in this study (ie., uWUE and TEA) rely on GPP estimates to obtain T, so any uncertainty resulting from NEE measurements, filtering, gap-filling, and partitioning would be inherently tied to our T, E, and T/ET estimates.

For one, the storage correction for CO_2 and energy fluxes was applied using only the one-point profile CO_2 storage estimate provided by Eddypro software. This could lead to an incorrect temporal attribution of fluxes and affect their partitioning (especially in the case of GPP). An underestimation of GPP may lead to an overestimation of T (through lower WUE). However, the lack of storage correction would also lead to an underestimation of LE fluxes, which could offset the lower GPP values and therefore partly compensate the effect on WUE and T estimation.

Moreover, we used a different partitioning method at the Amazon pasture site (daytime partitioning, Lasslop et al., 2010) because there was an insufficient relationship between ecosystem respiration and temperature that is necessary for the nighttime partitioning method (Reichstein et al., 2005). However, Nelson et al. (2020) found that the uncertainty introduced by the NEE partitioning method was small compared to the uncertainty introduced by the model used to partition ET, and the same was observed in this study ($T_{TEA\ NT} = 0.18 + 0.91T_{TEA\ DT}$, $R^2 = 0.87$) (Fig. S8). That T did not vary significantly by NEE partitioning method can be attributed to GPP not being used directly by the uWUE or TEA methods (it cancels out in the final step to estimate T, as $T = GPP/(GPP/T)$). Additionally, in the case of uWUE, some parameters are averaged or estimated using moving windows (Nelson et al., 2020), which could smooth some of the differences in GPP between both methods.

Another limitation comes from the energy balance closure problem when using the eddy covariance technique. Although eddy covariance is one of the best established methods to estimate ET and other trace gas fluxes at high temporal resolution (Baldocchi, 2014; Buysse et al., 2017; Pastorello et al., 2020; Wilson et al., 2001), the sum of sensible and latent heat fluxes ($H + LE$) measured via eddy covariance is generally not equal to the available energy (Rn – G), causing an 'energy balance' problem (Fisher et al., 2007; Hirschi et al., 2017; Pan et al., 2017) (Table S3). That is, H and LE can be underestimated by 10–30 % in EC studies (Wilson et al., 2001), with greater differences observed at sites with heterogeneous landscapes or during nighttime periods when there is generally low turbulence (Scott, 2010; Twine et al., 2000; Wilson et al., 2001). Although lower LE values would lead to an underestimation of all water fluxes (i.e., ET, T, and E), T/ET would likely remain consistent.

A final source of uncertainty is related to the ET partitioning method. Although the main seasonal patterns are consistent between partitioning methods (Scott et al., 2021), Nelson et al. (2020) showed that T/ET estimates from the uWUE method (mean site T/ET ~ 0.42) are lower than the current consensus that T/ET reflects the dominance of T as a terrestrial water flux (e.g., T/ET > 0.50). This was attributed to the use of the 75th and 95th percentiles to estimate the WUE (in the case of TEA and uWUE, respectively). Using a higher percentile may overestimate the WUE, and therefore underestimate T. Moreover, Nelson et al. (2020) stated that when using higher percentiles for TEA, the T values were similar in magnitude to the values from uWUE. In this study, we also observed that T_{TEA}/ET was generally higher than T_{uWUE}/ET ($T_{TEA}/ET = 0.32 + 0.71T_{uWUE}$, $R^2 = 0.39$, $p < 0.001$, Fig. S9). This could imply that the model needs to be adjusted to consider other parameters besides the optimization of carbon gain to water loss (De Kauwe et al., 2019; Nelson et al., 2020).

Overall, it has been reported that T/ET estimated using uWUE agrees more with sap-flow measurements, and that T/ET obtained via TEA is more consistent with the results obtained by Wei et al. (2017), although estimation of T remains unconstrained (Nelson et al., 2020).

As we focused on differences in patterns in ET, T and E across biomes and land-uses rather than the absolute magnitude of the fluxes, and because we treated all sites similarly, our results for the managed sites reflect the directions of hydrological changes resulting from land-use change. In the case of T/ET, we acknowledge that the estimate remains unconstrained for the region. Nevertheless, this study provides the first estimate of T/ET for several understudied sites, including seasonally dry Amazon forests, natural Cerrado savanna, and Pantanal ecosystems, as well as different land-uses within those biomes. This study also contributes information about the spatial and temporal variability of T/ET from these ecosystems following a consistent methodology across sites.

5. Conclusions

Overall, our study suggests that LULCC has a significant impact on ET, T, E, and T/ET in the region, by decreasing the magnitude and modifying the seasonality of these fluxes. In all studied biomes, managed sites showed a steeper decrease in ET and T during the dry season that was mostly driven by water stress, as crops and pasture were not able sustain higher transpiration rates compared to more deeply rooted natural sites that can access deeper water reserves. In addition, we found that in both Cerrado and Pantanal ecosystems there is a stronger stomatal control on water fluxes compared to natural Amazonian sites, particularly during the dry season. This study also provides information on T/ET for the understudied Pantanal and Cerrado biomes, and presents information on Amazon forests located in Southern Amazonia which could help better constraint T/ET at the global scale and help understand the surface-atmosphere exchanges of water and energy.

The results of this study are key for understanding how LULCC has affected the hydrology of the region. These findings can also be used to guide policies for better site management, as well as to inform climate models and obtain better predictions of what further changes in land-use and climate could mean for this region.

CRediT authorship contribution statement

B. D'Acunha: Conceptualization, Methodology, Data curation, Writing – original draft, Writing – review & editing, Visualization. **H.J. Dalmagro:** Conceptualization, Data curation, Writing – review & editing. **P.H. Zanella de Arruda:** Conceptualization, Writing – review & editing. **M.S. Biudes:** Writing – review & editing. **M.J. Lathuillière:** Conceptualization, Writing – review & editing. **M. Uribe:** Writing – review & editing. **E.G. Couto:** Conceptualization, Writing – review & editing. **P.M. Brando:** Writing – review & editing. **G. Vourlitis:** Conceptualization, Writing – review & editing. **M.S Johnson:** Conceptualization, Supervision, Writing – review & editing.

Declaration of Competing Interest

The authors declare that they have no known competing financial interests or personal relationships that could have appeared to influence the work reported in this paper.

Data availability

The data used in this study is available at DOI 10.5281/zenodo.7331957.

Supplementary materials

Supplementary material associated with this article can be found, in the online version, at doi:10.1016/j.agrformet.2023.109875.

References

Aybar, C., 2022. rgee: R bindings for calling the "Earth engine" API. J. Open Source Softw. Retrieved from https://github.com/r-spatial/rgee/.

Baker, J.C.A., Garcia-Carreras, L., Gloor, M., Marsham, J.H., Buermann, W., Da Rocha, H. R., Nobre, A.D., De Carioca Araujo, A., Spracklen, D.V., 2021. Evapotranspiration in the Amazon: spatial patterns, seasonality, and recent trends in observations, reanalysis, and climate models. Hydrol. Earth Syst. Sci. 25 (4), 2279–2300. https://doi.org/10.5194/hess-25-2279-2021.

Baker, J.C.A., Spracklen, D.V., 2019. Climate benefits of intact Amazon forests and the biophysical consequences of disturbance. Front. For. Glob. Change 2, 47. https://doi.org/10.3389/ffgc.2019.00047.

Balch, J.K., Nepstad, D.C., Brando, P.M., Curran, L.M., Portela, O., de Carvalho Jr., O., Lefebvre, P., 2008. Negative fire feedback in a transitional forest of southeastern Amazonia. Glob. Change Biol. 14 (10), 2276–2287.

Baldocchi, D., 2014. Measuring fluxes of trace gases and energy between ecosystems and the atmosphere - the state and future of the eddy covariance method. Glob. Chang. Biol. 20 (12), 3600–3609. https://doi.org/10.1111/gcb.12649.

Berkelhammer, M., Noone, D.C., Wong, T.E., Burns, S.P., Knowles, J.F., Kaushik, A., Blanken, P.D., Williams, M.W., 2016. Convergent approaches to determine an ecosystem's transpiration fraction. Global Biogeochem. Cycles 30 (6), 933–951. https://doi.org/10.1002/2016GB005392.

Brando, P.M., Silvério, D., Maracahipes-Santos, L., Oliveira-Santos, C., Levick, S.R., Coe, M.T., Migliavacca, M., Balch, J.K., Macedo, M.N., Nepstad, D.C., Maracahipes, L., 2019. Prolonged tropical forest degradation due to compounding disturbances: Implications for CO2 and H2O fluxes. Glob. Change Biol. 25 (9), 2855–2868.

Buysse, P., Bodson, B., Debacq, A., De Ligne, A., Heinesch, B., Manise, T., Moureaux, C., Aubinet, M., 2017. Carbon budget measurement over 12 years at a crop production site in the silty-loam region in Belgium. Agric. For. Meteorol. 246, 241–255. https://doi.org/10.1016/j.agrformet.2017.07.004.

Caballero, C.B., Ruhoff, A., Biggs, T., 2022. Land use and land cover changes and their impacts on surface-atmosphere interactions in Brazil: a systematic review. Sci. Total Environ. 808, 152134 https://doi.org/10.1016/j.scitotenv.2021.152134.

Cavalcante, R.B.L., Pontes, P.R.M., Souza-Filho, P.W.M., de Souza, E.B., 2019. Opposite effects of climate and land use changes on the annual water balance in the Amazon arc of deforestation. Water Resour. Res. 55 (4), 3092–3106. https://doi.org/10.1029/2019WR025083.

Chagas, V.B.P., Chaffe, P.L.B., Blöschl, G., 2022. Climate and land management accelerate the Brazilian water cycle. Nat. Commun. 13 (1), 5136. https://doi.org/10.1038/s41467-022-32580-x.

Choat, B., Jansen, S., Brodribb, T.J., Cochard, H., Delzon, S., Bhaskar, R., Bucci, S.J., Feild, T.S., Gleason, S.M., Hacke, U.G., Jacobsen, A.L., Lens, F., Maherali, H., Martínez-Vilalta, J., Mayr, S., Mencuccini, M., Mitchell, P.J., Nardini, A., Pittermann, J., Pratt, R.B., Sperry, J.S., Westoby, M., Wright, I.J., Zanne, A.E., 2012. Global convergence in the vulnerability of forests to drought. Nature 491 (7426), 752–755. https://doi.org/10.1038/nature11688.

Coenders-Gerrits, A.M.J., van der Ent, R.J., Bogaard, T.A., Wang-Erlandsson, L., Hrachowitz, M., Savenije, H.H.G., 2014. Uncertainties in transpiration estimates. Nature 506 (7487), E1–E2. https://doi.org/10.1038/nature12925.

Conte, L., Renner, M., Brando, P., Oliveira dos Santos, C., Silvério, D., Kolle, O., Trumbore, S.E., Kleidon, A., 2019. Effects of tropical deforestation on surface energy balance partitioning in Southeastern Amazonia estimated from maximum convective power. Geophys. Res. Lett. 46 (8), 4396–4403.

Costa, M.H., Biajoli, M.C., Sanches, L., Malhado, A.C.M., Hutyra, L.R., da Rocha, H.R., Aguiar, R.G., de Araújo, A.C., 2010. Atmospheric versus vegetation controls of Amazonian tropical rain forest evapotranspiration: are the wet and seasonally dry rain forests any different? J. Geophys. Res. 115 (G4), G04021. https://doi.org/10.1029/2009JG001179.

Cui, J., Tian, L., Wei, Z., Huntingford, C., Wang, P., Cai, Z., Ma, N., Wang, L., 2020. Quantifying the controls on evapotranspiration partitioning in the highest alpine meadow ecosystem. Water Resour. Res. 56 (4), e2019WR024815 https://doi.org/10.1029/2019WR024815.

Culf, A.D., Foken, T., Gash, J.H., 2004. The energy balance closure problem. In: Vegetation, Water, Humans and the Climate: A New Perspective on an Interactive System. Springer Berlin Heidelberg, Berlin, Heidelberg, pp. 159–166.

da Rocha, H.R., Manzi, A.O., Cabral, O.M., Miller, S.D., Goulden, M.L., Saleska, S.R., R-Coupe, N., Wofsy, S.C., Borma, L.S., Artaxo, P., Vourlitis, G., Nogueira, J.S., Cardoso, F.L., Nobre, A.D., Kruijt, B., Freitas, H.C., von Randow, C., Aguiar, R.G., Maia, J.F, 2009. Patterns of water and heat flux across a biome gradient from tropical forest to savanna in Brazil. J. Geophys. Res. 114 (1), G00B12. https://doi.org/10.1029/2007JG000640.

da Silva, J.B., Valle Junior, L.C.G., Faria, T.O., Marques, J.B., Dalmagro, H.J., Nogueira, J.S., Vourlitis, G.L., Rodrigues, T.R., 2021. Temporal variability in evapotranspiration and energy partitioning over a seasonally flooded scrub forest of the Brazilian Pantanal. Agric. For. Meteorol. 308-309, 108559 https://doi.org/10.1016/j.agrformet.2021.108559.

Dalmagro, H.J., Lathuillière, M.J., de Arruda, P.H.Z., Júnior, A.A.D.S., Sallo, F.D.S., Couto, E.G., Johnson, M.S., 2022. Carbon exchange in rainfed and irrigated cropland in the Brazilian Cerrado. Agric. For. Meteorol. 316, 108881.

Dalmagro, H.J., Lathuillière, M.J., Hawthorne, I., Morais, D.D., Pinto Jr, O.B., Couto, E. G., Johnson, M.S., Pinto, O.B., Couto, E.G., Johnson, M.S, 2018. Carbon biogeochemistry of a flooded Pantanal forest over three annual flood cycles. Biogeochemistry 139 (1), 1–18. https://doi.org/10.1007/s10533-018-0450-1.

Dalmagro, H.J., Zanella de Arruda, P.H., Vourlitis, G.L., Lathuillière, M.J., de, S., Nogueira, J., Couto, E.G., Johnson, M.S., 2019. Radiative forcing of methane fluxes offsets net carbon dioxide uptake for a tropical flooded forest. Glob. Chang. Biol. 25 (6), 1967–1981. https://doi.org/10.1111/gcb.14615.

Daughtry, C.S.T., Gallo, K.P., Goward, S.N., Prince, S.D., Kustas, W.P., 1992. Spectral estimates of absorbed radiation and phytomass production in corn and soybean canopies. Remote Sens. Environ. 39 (2), 141–152. https://doi.org/10.1016/0034-4257(92)90132-4.

De Kauwe, M.G., Medlyn, B.E., Pitman, A.J., Drake, J.E., Ukkola, A., Griebel, A., Pendall, E., Prober, S., Roderick, M., 2019. Examining the evidence for decoupling between photosynthesis and transpiration during heat extremes. Biogeosciences 16 (4), 903–916. https://doi.org/10.5194/bg-16-903-2019.

de Oliveira, J.V., Ferreira, D.B., da, S., Sahoo, P.K., Sodré, G.R.C., de Souza, E.B., Queiroz, J.C.B., 2018. Differences in precipitation and evapotranspiration between forested and deforested areas in the Amazon rainforest using remote sensing data. Environ. Earth Sci. 77 (6), 239. https://doi.org/10.1007/s12665-018-7411-9.

de Oliveira, R.G., Valle Júnior, L.C.G., da Silva, J.B., Espíndola, D.A.L.F., Lopes, R.D., Nogueira, J.S., Curado, L.F.A., Rodrigues, T.R., 2021. Temporal trend changes in reference evapotranspiration contrasting different land uses in southern Amazon basin. Agric. Water Manage. 250, 106815 https://doi.org/10.1016/j.agwat.2021.106815.

Efron, B., Tibshirani, R.J., 1994. An Introduction to the Bootstrap. CRC Press, New York.

Eichelmann, E., Mantoani, M.C., Chamberlain, S.D., Hemes, K.S., Oikawa, P.Y., Szutu, D., Valach, A., Verfaillie, J., Baldocchi, D.D., 2022. A novel approach to partitioning evapotranspiration into evaporation and transpiration in flooded ecosystems. Glob. Change Biol. 28 (3), 990–1007.

Fatichi, S., Pappas, C., 2017. Constrained variability of modeled T:ET ratio across biomes. Geophys. Res. Lett. 44 (13), 6795–6803. https://doi.org/10.1002/2017GL074041.

Fearnside, P.M., 2004. Environmental services as a basis for the sustainable use of tropical forests in Brazilian Amazonia. In: Proceedings of the *IV International Biennial Workshop Advances in Energy Studies: Energy-Ecology in Latin America.* Campinas, São Paulo, Brazil.

Fisher, J.B., Baldocchi, D.D., Misson, L., Dawson, T.E., Goldstein, A.H., 2007. What the towers don't see at night: nocturnal sap flow in trees and shrubs at two AmeriFlux sites in California. Tree Physiol. 27 (4), 597–610. https://doi.org/10.1093/treephys/27.4.597.

Fisher, J.B., Melton, F., Middleton, E., Hain, C., Anderson, M., Allen, R., McCabe, M.F., Hook, S., Baldocchi, D., Townsend, P.A., Kilic, A., Tu, K., Miralles, D.D., Perret, J., Lagouarde, J.P., Waliser, D., Purdy, A.J., French, A., Schimel, D., Famiglietti, J.S., Stephens, G., Wood, E.F., 2017. The future of evapotranspiration: global requirements for ecosystem functioning, carbon and climate feedbacks, agricultural management, and water resources. Water Resour. Res. 53, 2618–2626. https://doi.org/10.1002/2016WR020175.

Fisher, J.B., Whittaker, R.J., Malhi, Y., 2011. ET come home: potential evapotranspiration in geographical ecology. Global Ecol. Biogeogr. 20, 1–18. https://doi.org/10.1111/j.1466-8238.2010.00578.x.

Foken, T., Göockede, M., Mauder, M., Mahrt, L., Amiro, B., & Munger, W. (2006). Post-field data quality control. In *Handbook of Micrometeorology*. 10.1007/1-4020-2265-4_9.

Foken, T., 2008. The energy balance closure problem: An overview. Ecol. Appl. 18 (6), 1351–1367.

Fratini, G., Mauder, M., 2014. Towards a consistent eddy-covariance processing: an intercomparison of EddyPro and TK3. Atmos. Meas. Tech. 7 (7) https://doi.org/10.5194/amt-7-2273-2014.

Garcia, L.C., Szabo, J.K., de Oliveira Roque, F., de Matos Martins Pereira, A., Nunes da Cunha, C., Damasceno-Júnior, G.A., Morato, R.G., Tomas, W.M., Libonati, R., Ribeiro, D.B, 2021. Record-breaking wildfires in the world's largest continuous tropical wetland: integrative fire management is urgently needed for both biodiversity and humans. J. Environ. Manage. 293, 112870 https://doi.org/10.1016/j.jenvman.2021.112870.

Good, S.P., Noone, D., Bowen, G., 2015. Hydrologic connectivity constrains partitioning of global terrestrial water fluxes. Science 349 (6244). https://doi.org/10.1126/science.aaa5931.

Green, J.K., Berry, J., Ciais, P., Zhang, Y., Gentine, P., 2020. Amazon rainforest photosynthesis increases in response to atmospheric dryness. Sci. Adv. 6 (47), eabb7232. https://doi.org/10.1126/sciadv.abb7232.

Hirschi, M., Michel, D., Lehner, I., Seneviratne, S.I., 2017. A site-level comparison of lysimeter and eddy covariance flux measurements of evapotranspiration. Hydrol. Earth Syst. Sci. 21 (3), 1809–1825. https://doi.org/10.5194/hess-21-1809-2017.

Jaramillo, S., Graterol, E., Pulver, E., 2020. Sustainable transformation of rainfed to irrigated agriculture through water harvesting and smart crop management practices. Front. Sustain. Food Syst. 4, 437086 https://doi.org/10.3389/fsufs.2020.437086.

Jasechko, S., Sharp, Z.D., Gibson, J.J., Birks, S.J., Yi, Y., Fawcett, P.J., 2013. Terrestrial water fluxes dominated by transpiration. Nature 496 (7445), 347–350.

Keller, M., Silva-Dias, M.A., Nepstad, D.C., Andreae, M.O., 2004. The large-scale biosphere-atmosphere experiment in amazonia: analyzing regional land use change effects. Geophys. Monograph Ser. 153, 321–334. https://doi.org/10.1029/153GM24.

Kira, O., Nguy-Robertson, A.L., Arkebauer, T.J., Linker, R., Gitelson, A.A., 2016. Informative spectral bands for remote green LAI estimation in C3 and C4 crops. Agric. For. Meteorol. 218-219 https://doi.org/10.1016/j.agrformet.2015.12.064.

Knauer, J., El-Madany, T.S., Zaehle, S., Migliavacca, M., 2018. Bigleaf—an R package for the calculation of physical and physiological ecosystem properties from eddy covariance data. PLoS One 13 (8), e0201114. https://doi.org/10.1371/journal.pone.0201114.

Kundzewicz, Z.W., Mata, L.J., Arnell, N.W., DÖLL, P., Jimenez, B., Miller, K., Oki, T., ŞEN, Z., Shiklomanov, I, 2008. The implications of projected climate change for freshwater resources and their management. Hydrol. Sci. J. 53 (1), 3–10. https://doi.org/10.1623/hysj.53.1.3.

Lasslop, G., Reichstein, M., Papale, D., Richardson, A., Arneth, A., Barr, A., Stoy, P., Wohlfahrt, G., 2010. Separation of net ecosystem exchange into assimilation and respiration using a light response curve approach: critical issues and global evaluation. Glob. Chang. Biol. 16 (1), 187–208. https://doi.org/10.1111/j.1365-2486.2009.02041.x.

Lathuillière, M.J., Coe, M.T., Johnson, M.S., 2016. A review of green-and blue-water resources and their trade-offs for future agricultural production in the Amazon Basin: what could irrigated agriculture mean for Amazonia? Hydrol. Earth Syst. Sci. 20, 2179–2194. https://doi.org/10.5194/hess-20-2179-2016.

Lathuillière, M.J., Dalmagro, H.J., Black, T.A., Arruda, P.H.Z.de, Hawthorne, I., Couto, E. G., Johnson, M.S, 2018. Rain-fed and irrigated cropland-atmosphere water fluxes and their implications for agricultural production in Southern Amazonia. Agric. For. Meteorol. 256-257, 407–419. https://doi.org/10.1016/j.agrformet.2018.03.023.

Lathuillière, M.J., Johnson, M.S., Donner, S.D., 2012. Water use by terrestrial ecosystems: temporal variability in rainforest and agricultural contributions to evapotranspiration in Mato Grosso, Brazil. Environ. Res. Lett. 7 (2), 024024 https://doi.org/10.1088/1748-9326/7/2/024024.

Leopoldo, P.R., Franken, W.K., Villa Nova, N.A., 1995. Real evapotranspiration and transpiration through a tropical rain forest in central Amazonia as estimated by the water balance method. For. Ecol. Manage. 73 (1–3), 185–195. https://doi.org/10.1016/0378-1127(94)03487-H.

Levy, M.C., Lopes, A.V., Cohn, A., Larsen, L.G., Thompson, S.E., 2018. Land use change increases streamflow across the arc of deforestation in Brazil. Geophys. Res. Lett. 45 (8), 3520–3530. https://doi.org/10.1002/2017GL076526.

Loarie, S.R., Lobell, D.B., Asner, G.P., Field, C.B., Loarie, S.R., Lobell, D.B., Asner, G.P., Field, C.B., 2011. Land-cover and surface water change drive large albedo increases in South America*. Earth Interact. 15 (7), 1–16. https://doi.org/10.1175/2010EI342.1.

Longo, M., Saatchi, S., Keller, M., Bowman, K., Ferraz, A., Moorcroft, P.R., Morton, D.C., Bonal, D., Brando, P., Burban, B., Derroire, G., Dos-Santos, M.N., Meyer, V., Saleska, S., Trumbore, S., Vincent, G., 2020. Impacts of degradation on water, energy, and carbon cycling of the Amazon tropical forests. J. Geophys. Res. Biogeosci. 125 (8) https://doi.org/10.1029/2020JG005677.

Maeda, E.E., Ma, X., Wagner, F.H., Kim, H., Oki, T., Eamus, D., Huete, A., 2017. Evapotranspiration seasonality across the Amazon Basin. Earth Syst. Dyn. 8 (2), 439–454. https://doi.org/10.5194/esd-8-439-2017.

Mallick, K., Trebs, I., Boegh, E., Giustarini, L., Schlerf, M., Drewry, D.T., Hoffmann, L., Von Randow, C., Kruijt, B., Araùjo, A., Saleska, S., Ehleringer, J.R., Domingues, T.F., Ometto, J.P.H.B., Nobre, A.D., Luiz Leal De Moraes, O., Hayek, M., William Munger, J., Wofsy, S.C., 2016. Canopy-scale biophysical controls of transpiration and evaporation in the Amazon Basin. Hydrol. Earth Syst. Sci. 20 (10), 4237–4264. https://doi.org/10.5194/hess-20-4237-2016.

Marengo, J.A., Alves, L.M., Torres, R.R., 2016. Regional climate change scenarios in the Brazilian Pantanal watershed. Clim. Res. 68, 201–213. https://doi.org/10.3354/cr01324.

Melo, V.S., Desjardins, T., Silva Jr, M.L., Santos, E.R., Sarrazin, M., Santos, M.M.L.S, 2012. Consequences of forest conversion to pasture and fallow on soil microbial biomass and activity in the eastern Amazon. Soil Use Manag. 28 (4), 530–535. https://doi.org/10.1111/sum.12003.

Miralles, D.G., De Jeu, R.A.M., Gash, J.H., Holmes, T.R.H., Dolman, A.J., 2011. Magnitude and variability of land evaporation and its components at the global scale. Hydrol. Earth Syst. Sci. 15 (3), 967–981. https://doi.org/10.5194/hess-15-967-2011.

Montenegro, S., Ragab, R., 2012. Impact of possible climate and land use changes in the semi arid regions: a case study from North Eastern Brazil. J. Hydrol. 434-435 https://doi.org/10.1016/j.jhydrol.2012.02.036 *(Amst)*.

Myneni, R.B., Hoffman, S., Knyazikhin, Y., Privette, J.L., Glassy, J., Tian, Y., Wang, Y., Song, X., Zhang, Y., Smith, G.R., Lotsch, A., Friedl, M., Morisette, J.T., Votava, P., Nemani, R.R., Running, S.W., 2002. Global products of vegetation leaf area and fraction absorbed PAR from year one of MODIS data. Remote Sens. Environ. 83 (1–2), 214–231. https://doi.org/10.1016/S0034-4257(02)00074-3.

Nelson, J.A. (2020). *jnelson18/ecosystem-transpiration: Additional installation Instructions*. 10.5281/zenodo.3921923.

Nelson, J.A., Carvalhais, N., Cuntz, M., Delpierre, N., Knauer, J., Ogée, J., Migliavacca, M., Reichstein, M., Jung, M., 2018a. Coupling water and carbon fluxes to constrain estimates of transpiration: the TEA algorithm. J. Geophys. Res. Biogeosci. 123 (12), 3617–3632. https://doi.org/10.1029/2018JG004727.

Nelson, J.A., Carvalhais, N., Migliavacca, M., Reichstein, M., Jung, M., 2018b. Water-stress-induced breakdown of carbon-water relations: indicators from diurnal FLUXNET patterns. Biogeosciences 15 (8), 2433–2447. https://doi.org/10.5194/bg-15-2433-2018.

Nelson, J.A., Pérez-Priego, O., Zhou, S., Poyatos, R., Zhang, Y., Blanken, P.D., Gimeno, T. E., Wohlfahrt, G., Desai, A.R., Gioli, B., Limousin, J.M., Bonal, D., Paul-Limoges, E., Scott, R.L., Varlagin, A., Fuchs, K., Montagnani, L., Wolf, S., Delpierre, N., Berveiller, D., Gharun, M., Belelli Marchesini, L., Gianelle, D., Šigut, L., Mammarella, I., Siebicke, L., Andrew Black, T., Knohl, A., Hörtnagl, L., Magliulo, V., Besnard, S., Weber, U., Carvalhais, N., Migliavacca, M., Reichstein, M., Jung, M, 2020. Ecosystem transpiration and evaporation: insights from three water flux partitioning methods across FLUXNET sites. Glob. Chang. Biol. 26 (12), 6916–6930. https://doi.org/10.1111/gcb.15314.

Nepstad, D.C., de Carvalho, C.R., Davidson, E.A., Jipp, P.H., Lefebvre, P.A., Negreiros, G. H., da Silva, E.D., Stone, T.A., Trumbore, S.E., Vieira, S., 1994. The role of deep roots in the hydrological and carbon cycles of Amazonian forests and pastures. Nature 372 (6507), 666–669.

Nóbrega, R.L.B., Guzha, A.C., Torres, G.N., Kovacs, K., Lamparter, G., Amorim, R.S.S., Couto, E., Gerold, G., 2017. Effects of conversion of native cerrado vegetation to pasture on soil hydro-physical properties, evapotranspiration and streamflow on the Amazonian agricultural frontier. PLoS One. https://doi.org/10.1371/journal.pone.0179414.

Ohkubo, S., Hirano, T., Kusin, K., 2023. Influence of disturbance on transpiration and evaporation in tropical peat swamp forests. J. Hydrol. 620, 129523 https://doi.org/10.1016/j.jhydrol.2023.129523 *(Amst)*.

Oliveira, P.T.S., Wendland, E., Nearing, M.A., Scott, R.L., Rosolem, R., Da Rocha, H.R., 2015. The water balance components of undisturbed tropical woodlands in the Brazilian cerrado. Hydrol. Earth Syst. Sci. 19 (6), 2899–2910.

Paca, V.H.D.M., Espinoza-Dávalos, G.E., Hessels, T.M., Moreira, D.M., Comair, G.F., Bastiaanssen, W.G., 2019. The spatial variability of actual evapotranspiration across the Amazon River Basin based on remote sensing products validated with flux towers. Ecol. Process. 8 (1), 1–20.

Pan, X., Liu, Y., Fan, X., Gan, G., 2017. Two energy balance closure approaches: applications and comparisons over an oasis-desert ecotone. J. Arid. Land. 9 (1), 51–64. https://doi.org/10.1007/s40333-016-0063-2.

Papale, D., Reichstein, M., Aubinet, M., Canfora, E., Bernhofer, C., Kutsch, W., Longdoz, B., Rambal, S., Valentini, R., Vesala, T., Yakir, D., 2006. Towards a standardized processing of net ecosystem exchange measured with eddy covariance technique: algorithms and uncertainty estimation. Biogeosciences 3 (4), 571–583. https://doi.org/10.5194/bg-3-571-2006.

Paschalis, A., Fatichi, S., Pappas, C., Or, D., 2018. Covariation of vegetation and climate constrains present and future T/ET variability. Environ. Res. Lett. 13 (10), 104012 https://doi.org/10.1088/1748-9326/aae267.

Pastorello, G., Trotta, C., Canfora, E., Chu, H., Christianson, D., Cheah, Y.W., Poindexter, C., Chen, J., Elbashandy, A., Humphrey, M., Isaac, P., Polidori, D., Ribeca, A., van Ingen, C., Zhang, L., Amiro, B., Ammann, C., Arain, M.A., Ardö, J., Arkebauer, T., Arndt, S.K., Arriga, N., Aubinet, M., Aurela, M., Baldocchi, D., Barr, A., Beamesderfer, E., Marchesini, L.B., Bergeron, O., Beringer, J., Bernhofer, C., Berveiller, D., Billesbach, D., Black, T.A., Blanken, P.D., Bohrer, G., Boike, J., Bolstad, P.V., Bonal, D., Bonnefond, J.M., Bowling, D.R., Bracho, R., Brodeur, J., Brümmer, C., Buchmann, N., Burban, B., Burns, S.P., Buysse, P., Cale, P., Cavagna, M., Cellier, P., Chen, S., Chini, I., Christensen, T.R., Cleverly, J., Collalti, A., Consalvo, C., Cook, B.D., Cook, D., Coursolle, C., Cremonese, E., Curtis, P.S., D'Andrea, E., da Rocha, H., Dai, X., Davis, K.J., De Cinti, B., de Grandcourt, A., De Ligne, A., De Oliveira, R.C., Delpierre, N., Desai, A.R., Di Bella, C. M., di Tommasi, P., Dolman, H., Domingo, F., Dong, G., Dore, S., Duce, P., Dufrêne, E., Dunn, A., Dušek, J., Eamus, D., Eichelmann, U., ElKhidir, H.A.M., Eugster, W., Ewenz, C.M., Ewers, B., Famulari, D., Fares, S., Feigenwinter, I., Feitz, A., Fensholt, R., Filippa, G., Fischer, M., Frank, J., Galvagno, M., Gharun, M., Gianelle, D., Gielen, B., Gioli, B., Gitelson, A., Goded, I., Goeckede, M., Goldstein, A. H., Gough, C.M., Goulden, M.L., Graf, A., Griebel, A., Gruening, C., Grünwald, T., Hammerle, A., Han, S., Han, X., Hansen, B.U., Hanson, C., Hatakka, J., He, Y., Hehn, M., Heinesch, B., Hinko-Najera, N., Hörtnagl, L., Hutley, L., Ibrom, A., Ikawa, H., Jackowicz-Korczynski, M., Janouš, D., Jans, W., Jassal, R., Jiang, S., Kato, T., Khomik, M., Klatt, J., Knohl, A., Knox, S., Kobayashi, H., Koerber, G., Kolle, O., Kosugi, Y., Kotani, A., Kowalski, A., Kruijt, B., Kurbatova, J., Kutsch, W.L., Kwon, H., Launiainen, S., Laurila, T., Law, B., Leuning, R., Li, Y., Liddell, M., Limousin, J.M., Lion, M., Liska, A.J., Lohila, A., López-Ballesteros, A., López-Blanco, E., Loubet, B., Loustau, D., Lucas-Moffat, A., Lüers, J., Ma, S., Macfarlane, C., Magliulo, V., Maier, R., Mammarella, I., Manca, G., Marcolla, B., Margolis, H.A., Marras, S., Massman, W., Mastepanov, M., Matamala, R., Matthes, J.H., Mazzenga, F., McCaughey, H., McHugh, I., McMillan, A.M.S., Merbold, L., Meyer, W., Meyers, T., Miller, S.D., Minerbi, S., Moderow, U., Monson, R.K., Montagnani, L., Moore, C.E., Moors, E., Moreaux, V., Moureaux, C., Munger, J.W., Nakai, T., Neirynck, J., Nesic, Z., Nicolini, G., Noormets, A., Northwood, M., Nosetto, M., Nouvellon, Y., Novick, K., Oechel, W., Olesen, J.E., Ourcival, J.M., Papuga, S.A., Parmentier, F.J., Paul-Limoges, E., Pavelka, M., Peichl, M., Pendall, E., Phillips, R.P., Pilegaard, K., Pirk, N., Posse, G., Powell, T., Prasse, H., Prober, S.M., Rambal, S., Rannik, Ü., Raz-Yaseef, N., Reed, D., de Dios, V.R., Restrepo-Coupe, N., Reverter, B.R., Roland, M., Sabbatini, S., Sachs, T., Saleska, S.R., Sánchez-Cañete, E. P., Sanchez-Mejia, Z.M., Schmid, H.P., Schmidt, M., Schneider, K., Schrader, F., Schroder, I., Scott, R.L., Sedlák, P., Serrano-Ortíz, P., Shao, C., Shi, P., Shironya, I., Siebicke, L., Šigut, L., Silberstein, R., Sirca, C., Spano, D., Steinbrecher, R., Stevens, R.M., Sturtevant, C., Suyker, A., Tagesson, T., Takanashi, S., Tang, Y., Tapper, N., Thom, J., Tiedemann, F., Tomassucci, M., Tuovinen, J.P., Urbanski, S., Valentini, R., van der Molen, M., van Gorsel, E., van Huissteden, K., Varlagin, A., Verfaillie, J., Vesala, T., Vincke, C., Vitale, D., Vygodskaya, N., Walker, J.P., Walter-Shea, E., Wang, H., Weber, R., Westermann, S., Wille, C., Wofsy, S., Wohlfahrt, G., Wolf, S., Woodgate, W., Li, Y., Zampedri, R., Zhang, J., Zhou, G., Zona, D., Agarwal, D., Biraud, S., Torn, M., Papale, D, 2020. The FLUXNET2015 dataset and the ONEFlux processing pipeline for eddy covariance data. Sci. Data 7 (1), 225. https://doi.org/10.1038/s41597-020-0534-3.

Perez-Priego, O., Katul, G., Reichstein, M., El-Madany, T.S., Ahrens, B., Carrara, A., Scanlon, T.M., Migliavacca, M., 2018. Partitioning eddy covariance water flux components using physiological and micrometeorological approaches. J. Geophys. Res. Biogeosci. 123 (10), 3353–3370. https://doi.org/10.1029/2018JG004637.

Priante-Filho, N., Vourlitis, G.L., Hayashi, M.M.S., Nogueira, J.D.S., Campelo Jr., J.H., Nunes, P.C., Souza, L.S.E., Couto, E.G., Hoeger, W., Raiter, F., Trienweiler, J.L., 2004. Comparison of the mass and energy exchange of a pasture and a mature transitional tropical forest of the southern Amazon Basin during a seasonal transition. Glob. Change Biol. 10 (5), 863–876.

R Core Team, 2021. R core team (2021). R: A Language and Environment for Statistical Computing. R Foundation for Statistical Computing, Vienna, Austria. URL. Http://Www.R-Project.Org.

Reichstein, M., Falge, E., Baldocchi, D., Papale, D., Aubinet, M., Berbigier, P., Bernhofer, C., Buchmann, N., Gilmanov, T., Granier, A., Grunwald, T., Havrankova, K., Ilvesniemi, H., Janous, D., Knohl, A., Laurila, T., Lohila, A., Loustau, D., Matteucci, G., Meyers, T., Miglietta, F., Ourcival, J.-M., Pumpanen, J., Rambal, S., Rotenberg, E., Sanz, M., Tenhunen, J., Seufert, G., Vaccari, F., Vesala, T., Yakir, D., Valentini, R., 2005. On the separation of net ecosystem exchange into assimilation and ecosystem respiration: review and improved algorithm. Glob. Chang. Biol. 11 (9), 1424–1439. https://doi.org/10.1111/j.1365-2486.2005.001002.x.

Restrepo-Coupe, N., da Rocha, H.R., Hutyra, L.R., da Araujo, A.C., Borma, L.S., Christoffersen, B., Cabral, O.M.R., de Camargo, P.B., Cardoso, F.L., da Costa, A.C.L., Fitzjarrald, D.R., Goulden, M.L., Kruijt, B., Maia, J.M.F., Malhi, Y.S., Manzi, A.O., Miller, S.D., Nobre, A.D., von Randow, C., Sá, L.D.A., Sakai, R.K., Tota, J., Wofsy, S. C., Zanchi, F.B., Saleska, S.R., 2013. What drives the seasonality of photosynthesis across the Amazon basin? A cross-site analysis of eddy flux tower measurements from the Brasil flux network. Agric. For. Meteorol. 182-183, 128–144. https://doi.org/10.1016/j.agrformet.2013.04.031.

Restrepo-Coupe, N., Levine, N.M., Christoffersen, B.O., Albert, L.P., Wu, J., Costa, M.H., Galbraith, D., Imbuzeiro, H., Martins, G., da Araujo, A.C., Malhi, Y.S., Zeng, X., Moorcroft, P., Saleska, S.R., 2017. Do dynamic global vegetation models capture the seasonality of carbon fluxes in the Amazon basin? A data-model intercomparison. Glob. Chang. Biol. 23 (1), 191–208. https://doi.org/10.1111/gcb.13442.

Rockström, J., 2003. Water for food and nature in drought-prone tropics: vapour shift in rain-fed agriculture. Philosoph. Trans. R. Soc. B Biol. Sci. 358 (1440), 1997–2009. https://doi.org/10.1098/RSTB.2003.1400.

Salati, E., Vose, P.B., 1984. Amazon Basin: a System in Equilibrium. Science 225 (4658), 129–138. https://doi.org/10.1126/science.225.4658.129.

Salazar, A., Baldi, G., Hirota, M., Syktus, J., McAlpine, C., 2015. Land use and land cover change impacts on the regional climate of non-Amazonian South America: a review. Glob. Planet Change 128, 103–119. https://doi.org/10.1016/j.gloplacha.2015.02.009.

Scanlon, T.M., Kustas, W.P., 2010. Partitioning carbon dioxide and water vapor fluxes using correlation analysis. Agric. For. Meteorol. 150 (1), 89–99. https://doi.org/10.1016/j.agrformet.2009.09.005.

Schlesinger, W.H., Jasechko, S., 2014. Transpiration in the global water cycle. Agric. For. Meteorol. 189-190 https://doi.org/10.1016/j.agrformet.2014.01.011.

Scott, R.L., 2010. Using watershed water balance to evaluate the accuracy of eddy covariance evaporation measurements for three semiarid ecosystems. Agric. For. Meteorol. 150 (2), 219–225. https://doi.org/10.1016/J.AGRFORMET.2009.11.002.

Scott, R.L., Biederman, J.A., 2017. Partitioning evapotranspiration using long-term carbon dioxide and water vapor fluxes. Geophys. Res. Lett. 44 (13), 6833–6840. https://doi.org/10.1002/2017GL074324.

Scott, R.L., Knowles, J.F., Nelson, J.A., Gentine, P., Li, X., Barron-Gafford, G., Bryant, R., Biederman, J.A., 2021. Water Availability Impacts on Evapotranspiration Partitioning. Agric. For. Meteorol. 297, 108251 https://doi.org/10.1016/j.agrformet.2020.108251.

Shuttleworth, W.J., 1988. Evaporation from Amazonian rainforest. Proc. R. Soc. Lond. B Biol. Sci. 233 (1272), 321–346. https://doi.org/10.1098/rspb.1988.0024.

Signori-Müller, C., Oliveira, R.S., Barros, F.de V., Tavares, J.V., Gilpin, M., Diniz, F.C., Zevallos, M.J.M., Yupayccana, C.A.S., Acosta, M., Bacca, J., Chino, R.S.C., Cuellar, G. M.A., Cumapa, E.R.M., Martinez, F., Mullisaca, F.M.P., Nina, A., Sanchez, J.M.B., da Silva, L.F., Tello, L., Tintaya, J.S., Ugarteche, M.T.M., Baker, T.R., Bittencourt, P.R. L., Borma, L.S., Brum, M., Castro, W., Coronado, E.N.H., Cosio, E.G., Feldpausch, T. R., Fonseca, L.d'A.M., Gloor, E., Llampazo, G.F., Malhi, Y., Mendoza, A.M., Moscoso, V.C., Araujo-Murakami, A., Phillips, O.L., Salinas, N., Silveira, M., Talbot, J., Vasquez, R., Mencuccini, M., Galbraith, D, 2021. Non-structural carbohydrates mediate seasonal water stress across Amazon forests. Nat. Commun. 12 (1), 1–9. https://doi.org/10.1038/s41467-021-22378-8.

Skaggs, T.H., Anderson, R.G., Alfieri, J.G., Scanlon, T.M., Kustas, W.P., 2018. Fluxpart: open source software for partitioning carbon dioxide and water vapor fluxes. Agric. For. Meteorol. 253-254 https://doi.org/10.1016/j.agrformet.2018.02.019.

Staal, A., Flores, B.M., Aguiar, A.P.D., Bosmans, J.H.C., Fetzer, I., Tuinenburg, O.A., 2020. Feedback between drought and deforestation in the Amazon. Environ. Res. Lett. 15 (4), 044024 https://doi.org/10.1088/1748-9326/ab738e.

Sterling, S.M., Ducharne, A., Polcher, J., 2012. The impact of global land-cover change on the terrestrial water cycle. Nat. Clim. Chang. 3 (4), 385–390. https://doi.org/10.1038/nclimate1690. *2012 3:4*.

Sun, X., Wilcox, B.P., Zou, C.B., 2019. Evapotranspiration partitioning in dryland ecosystems: A global meta-analysis of in situ studies. J. Hydrol. 576, 123–136.

Twine, T.E., Kustas, W.P., Norman, J.M., Cook, D.R., Houser, P.R., Meyers, T.P., Prueger, J.H., Starks, P.J., Wesely, M.L., 2000. Correcting eddy-covariance flux underestimates over a grassland. Agric. For. Meteorol. 103 (3), 279–300. https://doi.org/10.1016/S0168-1923(00)00123-4.

Uribe, M., del, R., Dukes, J.S., 2021. Land cover change alters seasonal photosynthetic activity and transpiration of Amazon forest and Cerrado. Environ. Res. Lett. 16 (5), 054013 https://doi.org/10.1088/1748-9326/abf60d.

Vourlitis, G.L., Filho, N.P., Hayashi, M.M.S., de, S., Nogueira, J., Caseiro, F.T., Campelo, J.H., 2002. Seasonal variations in the evapotranspiration of a transitional tropical forest of Mato Grosso, Brazil. Water Resour. Res. 38 (6), 30. https://doi.org/10.1029/2000WR000122. -1-30–11.

Vourlitis, G.L., Priante Filho, N., Hayashi, M.M., Nogueira, J.D.S., Raiter, F., Hoegel, W., Campelo Jr., J.H., 2004. Effects of meteorological variations on the CO2 exchange of a Brazilian transitional tropical forest. Ecol. Appl. 14 (sp4), 89–100.

Vourlitis, G.L., de Souza Nogueira, J., Priante Filho, N., Hoeger, W., Raiter, F., Biudes, M. S., Arruda, J.C., Capistrano, V.B., de Faria, J.L.B., de Almeida Lobo, F., 2005. The sensitivity of diel CO2 and H2O vapor exchange of a tropical transitional forest to seasonal variation in meteorology and water availability. Earth Interact. 9 (27), 1–23.

Vourlitis, G.L., de Souza Nogueira, J., de Almeida Lobo, F., Sendall, K.M., de Paulo, S.R., Antunes Dias, C.A., Pinto Jr., O.B., de Andrade, N.L.R., 2008. Energy balance and canopy conductance of a tropical semi-deciduous forest of the southern Amazon Basin. Water Resour. Res. 44 (3) https://doi.org/10.1029/2006WR005526.

Vourlitis, G.L., de Almeida Lobo, F., Zeilhofer, P., de Souza Nogueira, J., 2011. Temporal patterns of net CO2 exchange for a tropical semideciduous forest of the southern Amazon Basin. J. Geophys. Res. Biogeosci. 116 (G3) https://doi.org/10.1029/2010JG001524.

Vourlitis, G.L., de Souza Nogueira, J., de Almeida Lobo, F., Pinto, O.B., 2015. Variations in evapotranspiration and climate for an Amazonian semi-deciduous forest over seasonal, annual, and El Niño cycles. Int. J. Biometeorol. 59 (2), 217–230. https://doi.org/10.1007/s00484-014-0837-1.

Wang, L., Good, S.P., Caylor, K.K., 2014. Global synthesis of vegetation control on evapotranspiration partitioning. Geophys. Res. Lett. 41 (19), 6753–6757. https://doi.org/10.1002/2014GL061439.

Wei, Z., Yoshimura, K., Wang, L., Miralles, D.G., Jasechko, S., Lee, X., 2017. Revisiting the contribution of transpiration to global terrestrial evapotranspiration. Geophys. Res. Lett. 44 (6), 2792–2801. https://doi.org/10.1002/2016GL072235.

Wilson, K., Goldstein, A., Falge, E., Aubinet, M., Baldocchi, D., Berbigier, P., Bernhofer, C., Ceulemans, R., Dolman, H., Field, C., Grelle, A., 2002. Energy balance closure at FLUXNET sites. Agric. For. Meteorol. 113 (1–4), 223–243.

Wilson, K., Hanson, P.J., Mulholland, P.J., Baldocchi, D.D., Wullschleger, S.D., 2001. A comparison of methods for determining forest evapotranspiration and its components: sap-flow, soil water budget, eddy covariance and catchment water balance. Agric. For. Meteorol. 106 (2), 153–168. https://doi.org/10.1016/S0168-1923(00)00199-4.

Wu, J., Lakshmi, V., Wang, D., Lin, P., Pan, M., Cai, X., Wood, E.F., Zeng, Z., 2020. The reliability of global remote sensing evapotranspiration products over Amazon. Remote Sens. 12 (14), 2211. https://doi.org/10.3390/rs12142211 *(Basel)*.

Wutzler, T., Lucas-Moffat, A., Migliavacca, M., Knauer, J., Sickel, K., Šigut, L., Menzer, O., Reichstein, M., 2018. Basic and extensible post-processing of eddy covariance flux data with REddyProc. Biogeosciences 15 (16), 5015–5030. https://doi.org/10.5194/bg-15-5015-2018.

Xu, D., Agee, E., Wang, J., Ivanov, V.Y., 2019. Estimation of Evapotranspiration of Amazon rainforest using the maximum entropy production method. Geophys. Res. Lett. 46 (3), 1402–1412. https://doi.org/10.1029/2018GL080907.

Zanella De Arruda, P.H., Vourlitis, G.L., Santanna, F.B., Pinto Jr., O.B., De Almeida Lobo, F., De Souza Nogueira, J., 2016. Large net CO2 loss from a grass-dominated tropical savanna in south-central Brazil in response to seasonal and interannual drought. J. Geophys. Res. Biogeosci. 121 (8), 2110–2124.

Zemp, D.C., Schleussner, C.F., Barbosa, H.M.J., Van Der Ent, R.J., Donges, J.F., Heinke, J., Sampaio, G., Rammig, A., 2014. On the importance of cascading moisture recycling in South America. Atmos. Chem. Phys. 14, 13337–13359. https://doi.org/10.5194/acp-14-13337-2014.

Zhou, S., Yu, B., Zhang, Y., Huang, Y., Wang, G., 2016. Partitioning evapotranspiration based on the concept of underlying water use efficiency. Water Resour. Res. 52 (2) https://doi.org/10.1002/2015WR017766.

Zhou, S., Yu, B., Zhang, Y., Huang, Y., Wang, G., 2018. Water use efficiency and evapotranspiration partitioning for three typical ecosystems in the Heihe River Basin, northwestern China. Agric. For. Meteorol. 253-254, 261–273. https://doi.org/10.1016/j.agrformet.2018.02.002.